

國立交通大學

電子工程學系

電子研究所碩士班

碩士論文

碘乙烷催化劑對銅化學氣相沉積特性之影響

Effects of C_2H_5I Catalyst on the Property of Cu Chemical Vapor Deposition

研究生：王安志

指導教授：陳茂傑

中華民國九十三年七月

碘乙烷催化劑對銅化學氣相沉積特性之影響

Effects of C₂H₅I Catalyst on the Property of Cu Chemical Vapor Deposition

研究生：王安志

Student : Wang, An-Chih

指導教授：陳茂傑

Advisor : Chen, Mao-Chieh



A Thesis

Submitted to Department of Electronics Engineering &
Institute of Electronics
College of Electrical Engineering and Computer Science
National Chiao Tung University
in partial Fulfillment of the Requirements
for the Degree of
Master
in
Electronics Engineering
July 2004

Hsinchu, Taiwan, Republic of China

碘乙烷催化劑對銅化學氣相沉積特性之影響

研究生：王安志

指導教授：陳茂傑

國立交通大學

電子工程學系 電子研究所碩士班

摘要

本論文使用自行組建之多腔體式低壓銅化學氣相沉積(Cu CVD)系統，以Cu(hfac)TMVS+2.4wt% TMVS當作先驅物(precursor)，探討以碘乙烷(C₂H₅I)作為催化劑對TaN基板做前處理，對銅膜沉積過程、銅膜性質以及管洞填充所產生的影響。催化劑的基板前處理係以濺鍍成長的TaN基板在定溫定壓條件下，暴露在碘乙烷的蒸氣之下三分鐘。由於附著在基板上的碘原子具有促進Cu(hfac)分解的作用，因此銅的成核率變快；再者，可能由於基板的表面能減小或銅膜與基板之間的介面能增加，使得銅核顆粒的接觸角(contact angle or wetting angle)變大。實驗結果發現，銅膜在碘乙烷處理過之TaN基板上具有較高的沉積速率、較低的電阻率、以及較強度的Cu(200)晶向成長傾向，但銅膜對基板的附著力則變差。銅膜沉積後在氮氣中施以 400°C的後續退火處理可進一步降低銅膜的電阻率，並且改善銅膜表面的粗糙度。到目前的實驗結果顯示，碘乙烷處理對於Cu CVD的管洞填充能力並沒有明顯的改善，但是實驗結果也證實低溫低壓以及高濃度含銅氣氛有利於提昇Cu CVD的填洞能力。

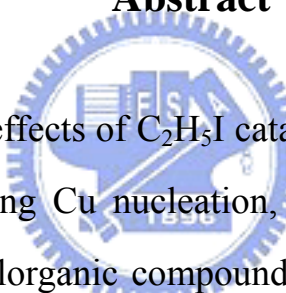
Effects of C_2H_5I Catalyst on the Property of Cu Chemical Vapor Deposition

Student: Wang, An-Chih

Advisor: Chen, Mao-Chieh

Institute of Electronics
Department of Electronics Engineering
National Chiao Tung University

Abstract



This thesis studies the effects of C_2H_5I catalyst on the copper chemical vapor deposition (Cu CVD), including Cu nucleation, Cu film property, and via-filling capability, using a liquid metalorganic compound of Cu(hfac)TMVS with 2.4 wt% TMVS additive as the precursor. Sputter-deposited TaN was used as the substrate for the Cu CVD and the vapor phase C_2H_5I was used for TaN surface treatment prior to the Cu CVD. The substrate pretreatment by C_2H_5I enhanced the adsorption of Cu species on the substrate surface, reduced the incubation time of nucleation, and thus accelerated the Cu film formation. The wetting angle of Cu grains nucleated on the C_2H_5I -treated TaN substrate surface was larger than that nucleated on the control TaN substrate (63° vs. 94°), presumably due to the increase of substrate surface energy and/or the decrease of Cu/substrate interfacial energy. The Cu films deposited on the C_2H_5I -treated TaN substrate all exhibited higher growth rate and lower electrical resistivity; however, they all exhibited a lower intensity peak ratio of Cu(111) to Cu(200) reflections and a degraded adhesion to the TaN substrate.

Post-deposition thermal annealing at 400°C in N₂ ambient was able to further reduce the film resistivity and surface roughness. Via-filling capability of Cu CVD by using vapor phase C₂H₅I substrate pretreatment did not exhibit an obvious improvement. However, it was found that notable improvement in via-filling capability of Cu CVD can be achieved at low deposition temperature, low deposition pressure, and high concentration of precursor species in the gas phase of CVD.



誌謝

碩士班的兩年，真的是一下就過去了，明明覺得才剛從大學的畢業旅行回來而已...相較於其他同學碩士班時的辛勞，也許我是算過得相當愜意的吧！這一切的一切，最要感謝的就是我最敬愛的陳茂傑老師了。老師在研究方面給了我高度的自主性，讓我在沒有壓力的情況下照著自己的步調做實驗，而使我在做研究之餘，也能擁有自己的生活。此外，在實驗遇到問題時，老師也總是會提出適時的建議，讓我不至於迷失了研究方向。而老師對於論文的嚴謹要求，更是讓我體會到了做事的正確態度。這一切的一切都使我獲益良多。

感謝林成利學長以及張君禮學長在這兩年間幫助我解決了許多機台上的問題，讓我得以順利完成這本論文，可謂是前人種樹，後人乘涼，學長真是功德無量。感謝實驗室的學長們：王超群學長的熱心幫忙，以及蔣秋志學長和吳偉豪學長每每在開會時提出的建言，讓果感受到了學長學弟間溫暖的情誼。感謝林信宏、柯依秀以及楊宇國，不僅平常和我說說笑笑，在我需要幫忙時也是二話不說，真的是一群大好人。王大榮、杜長慶是我研究所兩年來的好室友，因為有他們，我才能快樂的渡過這兩年，我會懷念一起吃宵夜和打 NBA 的時光的，真的非常感謝。一定要感謝的是我的爸媽和哥哥，他們一直以來給我支持與溫暖。最後我要感謝苑真，讓我學生生涯的最後一個學期，成為我最快樂的一個學期。

Contents

Abstract (Chinese)	i
Abstract (English)	ii
Acknowledgment (Chinese)	iv
Contents	v
Table Captions	vii
Figure Captions	viii
Chapter 1 Introduction	
1.1 General Background.....	1
1.2 Why use Cu-CVD.....	2
1.3 The Catalyst Surfactant of C ₂ H ₅ I.....	2
1.4 Thesis Organization.....	3
Chapter 2 Multi-Chamber Cu CVD System and Cu Precursor	
2.1 Multi-Chamber Low Pressure Cu CVD System.....	5
2.2 Real-time Automatic Monitor and Controller System.....	8
2.3 Reaction of Cu precursor.....	8
Chapter 3 Nucleation of Cu Using Iodoethane as Catalyst	
3.1 Introduction.....	21
3.2 Experimental Details.....	21
3.3 Results and Discussion.....	22
3.4 Summary.....	25
Chapter 4 CVD Cu Films on C₂H₅I –Treated TaN Substrate	

4.1 Introduction.....	31
4.2 Experimental Details.....	31
4.3 Effect of TaN Substrate Treatment by C ₂ H ₅ I on CVD Cu Films...	32
4.4 Effect of Post-Deposition Thermal Annealing.....	35
4.5 Summary.....	36
Chapter 5 Via-Filling of Cu CVD on Via-Patterned Substrate with TaN Liner	
5.1 Introduction.....	55
5.2 Experimental Details.....	55
5.3 Via-Filling on Via-Patterned Substrate with TaN Liner.....	56
5.4 Effect of C ₂ H ₅ I treatment on Via-Filling.....	58
5.5 Summary.....	58
Chapter 6 Conclusion and Suggestions for Future Work	
6.1 Conclusion.....	64
6.2 Suggestions for Future Work.....	65
References.....	66

Table Captions

Chapter 3

Table 3-1 Major parameters and processing conditions of Cu CVD used in this study.

Chapter 4

Table 4-1 Results of Scotch tape pulling test on the adhesion of CVD Cu films to TaN substrate.

Table 4-2 Effect of thermal annealing (400°C in N₂ for 30 min) on resistivity for Cu films deposited on TaN substrates with/without C₂H₅I treatment.



Figure Captions

Chapter 1

Fig. 1-1 Intrinsic gate delay vs. interconnect RC delay at minimum design rules of each technology node.

Chapter 2

Fig. 2-1 Schematic diagram of the multi-chamber low pressure CVD system used in the study of this thesis.

Fig. 2-2 The panorama photograph of the multi-chamber Cu CVD apparatus.

Fig. 2-3 Photograph showing the cluster-chamber, DLI system, and gas piping system.

Fig. 2-4 Photograph showing the robot arm in the transfer chamber.

Fig. 2-5 Schematic diagram of the pretreatment chamber.

Fig. 2-6 Schematic diagram of the reaction chamber (copper deposition chamber).

Fig. 2-7 Schematic diagram of the direct liquid injection (DLI) precursor delivery system.

Fig. 2-8 Schematic diagram of the catalyst storage and injection system.

Fig. 2-9 Schematic diagram of the automatic remote monitor and controller (ARMC) system, which is composed of a host computer, a subsidiary controller, and a unit controller of the Cu CVD apparatus.

Fig. 2-10 The friendly monitor and control program displays in the host computer screen.

Fig. 2-11 The deposition mechanism of Cu film by Cu(hfac)TMVS precursor.

Chapter 3

Fig. 3-1 Top view SEM micrographs showing Cu grain nucleation on control TaN substrate

Fig. 3-2 Top view SEM micrographs showing Cu grain nucleation on C₂H₅I-treated TaN substrate for (a) 1 min, (b) 2 min, and (c) 3 min of Cu-CVD.

Fig. 3-3 Schematic illustration of Cu nucleation and Young's equation.

Fig. 3-4 Oblique view SEM micrographs showing Cu grain nucleation for (a) 3 min on as-deposited and (b) 1 min on C₂H₅I-treated TaN substrates.

Chapter 4

Fig. 4-1 Effective deposition rate vs. substrate temperature (Arrhenius plot) for Cu films deposited at a pressure of 150 mtorr on TaN substrate with and without C₂H₅I treatment.

Fig. 4-2 SEM micrograph showing surface morphology of Cu film deposited on C₂H₅I-treated TaN substrate at 200°C.

Fig. 4-3 Resistivity vs. deposition temperature for Cu films deposited at a pressure of 150 mtorr on TaN substrate with and without C₂H₅I treatment.

Fig. 4-4 SEM micrographs showing surface morphology of Cu films deposited on control TaN substrate at (a) 140°C, (b) 160°C, (c) 180°C, (d) 200°C, (e) 220°C, and (f) 240°C.

Fig. 4-5 SEM micrographs showing surface morphology of Cu films deposited on C₂H₅I-treated TaN substrate at (a) 140°C, (b) 160°C, and (c) 180°C.

Fig. 4-6 XRD spectra of Cu films deposited on control TaN substrate at different temperatures.

Fig. 4-7 XRD spectra of Cu films deposited on C₂H₅I-treated TaN substrate at different temperatures.

Fig. 4-8 AFM image showing surface roughness for Cu films deposited in a duration of 10 min on control TaN substrate at different temperatures.

Fig. 4-9 AFM image showing surface roughness for Cu films deposited in a duration of 10 min on C₂H₅I-treated TaN substrate at different temperatures.

Fig. 4-10 SEM micrographs showing surface morphology of 400°C-annealed Cu films deposited on control TaN substrate at (a) 140°C, (b) 160°C, (c) 180°C, (d) 200°C, (e) 220°C, and (f) 240°C.

Fig. 4-11 SEM micrographs showing surface morphology of 400°C-annealed Cu films deposited on C₂H₅I-treated TaN substrate at (a) 140°C, (b) 160°C, and (c) 180°C.

Fig. 4-12 AFM image showing surface roughness of 400°C-annealed Cu films deposited on control TaN substrate at different temperatures.

Fig. 4-13 AFM image showing surface roughness of 400°C-annealed Cu films deposited on C₂H₅I-treated TaN substrate at different temperatures.

Fig. 4-14 Improvement of surface roughness vs. deposition temperature for Cu films deposited on TaN substrate with and without C₂H₅I treatment after 400°C thermal annealing.

Fig. 4-15 XRD spectra of 400°C-annealed Cu films deposited on control TaN substrate at different temperatures.

Fig. 4-16 XRD spectra of 400°C-annealed Cu films deposited on C₂H₅I-treated TaN substrate at different temperatures.

Chapter 5

Fig. 5-1 SEM micrographs showing cross-sectional views of via-filling for 0.25- μm -diameter vias under 150 mtorr at (a) 140°C, (b) 160°C, (c) 180°C, and (d) 200°C. The Cu CVD was conducted for 10 min for all samples.

Fig. 5-2 SEM micrographs showing cross-sectional views of via-filling for 0.16- μm -diameter vias under 150 mtorr at (a) 140°C, (b) 160°C, (c) 180°C, and (d) 200°C. The Cu CVD was conducted for 10 min for all samples.

Fig. 5-3 SEM micrographs showing cross-sectional views of via-filling for 0.16- μm -diameter vias under 60 mtorr at (a) 140°C, and (b) 160°C. The Cu CVD was conducted for 10 min.

Fig. 5-4 SEM micrographs showing cross-sectional views of via-filling for 0.16- μm -diameter vias on $\text{C}_2\text{H}_5\text{I}$ -treated patterned substrate under 150 mtorr at (a) 140°C, (b) 160°C, (c) 180°C, and (d) 200°C. The Cu CVD was conducted for 10 min for all samples.

Fig. 5-5 SEM micrographs showing cross-sectional views of via-filling for 0.16- μm -diameter vias on $\text{C}_2\text{H}_5\text{I}$ -treated patterned substrate under 60 mtorr at (a) 140°C, and (b) 160°C. The Cu CVD was conducted for 10 min.

Chapter 1

Introduction

1.1 General Background

As the devices feature size in the integrated circuits continuously scales down, the speed of devices is getting faster and faster, whereas the interconnect RC delay is becoming the dominant factor in determining the operation speed of the integrated circuits, as shown in Fig. 1-1 [1]. To reduce the interconnect RC time delay, copper (Cu) has been used in recent years to replace the conventional Al and Al-alloy as interconnect material in deep sub-quarter-micron regime because of its lower bulk electrical resistivity ($1.68\mu\Omega\text{-cm}$ for Cu vs. $2.66\mu\Omega\text{-cm}$ for Al and $> 3.0\mu\Omega\text{-cm}$ for Al-alloys), superior resistance to electromigration, higher resistance to stress-induced voids, higher melting point (1085°C for Cu vs. 660°C for Al), and better thermal conductivity (3.98 W/cm for Cu vs. 2.98 W/cm for Al) [2-7].

However, Cu also suffers from a number of drawbacks in its applications to the Si-based microelectronic technology as follows. Cu lacks the dry etching process, which is of vital importance to the success of sub-micron integrated circuits. Cu readily diffuses into Si substrate, causing the formation of deep-level traps and thus the degradation of device characteristics. Cu also forms Cu-Si compounds at temperatures as low as 200°C . Moreover, Cu readily drifts in oxide layer under the applied electric field [8-12]. As a result, Cu damascene scheme has been developed to cope with the difficult dry etching problem of Cu, and various barrier layers have been employed to prevent Cu from diffusing into its

surrounding oxide/dielectric layers and devices active regions.

1.2 Why use Cu CVD?

Cu films can be deposited by a number of methods, such as electrochemical deposition (ECD), sputtering (physical vapor deposition, PVD), and chemical vapor deposition (CVD). Electrochemical deposition, such as electroplating, is widely used in microelectronic industry. However, this method needs a conformal thin Cu film as a seed layer to promote nucleation and film growth. The step coverage of the thin seed layer is of vital importance to the success of gap-filling for the miniature vias and trenches. The Cu seed layers are usually sputter deposited (i.e. PVD). However, when the feature size of vias and trenches becomes smaller and smaller, PVD is no longer capable of providing a good enough step coverage for the via- or trench-filling process. The method of CVD inherently possesses a superior conformal film deposition. Moreover, it was reported recently that the inclusion of certain additives in the Cu CVD process resulted in via-filling of Cu in a bottom-up fashion [13]. This seems to make the Cu-CVD possibly a potential mainstream Cu-film deposition method in future microelectronic technology.

1.3 The Catalyst Surfactant of C₂H₅I

Recently, there have been a number of reports in literature concerning the effects of iodine (I) atom on the process of Cu-CVD [13-16]. Several organic catalysts, such as CH₂I₂ and C₂H₅I, have been used to investigate the effects of iodine. It was reported that iodine atoms on the substrate surface decrease the incubation time, increase the deposition rate and improve the surface roughness

of Cu films [15,16]. Moreover, iodine atoms promote the bottom-up fashion in the deep sub-micron via/trench filling process. Similar effect was observed for other catalysts that provide iodine atoms in the Cu CVD process [15]. In this thesis study, C_2H_5I is used as the catalyst for Cu CVD because of its facility of handling. C_2H_5I has a high vapor pressure at room temperature (137.52 mmHg at 25°C); thus, iodine vapor is readily available to be easily guided into the reaction chamber of CVD system.

1.4 Thesis Organization

This thesis consists of six chapters. Following the introduction in chapter 1, chapter 2 presents in detail the low-pressure CVD system used for this thesis work. Chapters 3, 4 and 5 contain the major results of this thesis study. Chapter 3 deals with the effect of iodine on the characteristics of Cu nucleation and film growth. In chapter 4, we characterize the Cu films deposited using iodine as a catalyst. Chapter 5 contains the study on the via-filling capability of Cu-CVD using the iodoethane (C_2H_5I) additive. Finally, chapter 6 gives the conclusion of this thesis work and the suggestions for future study.

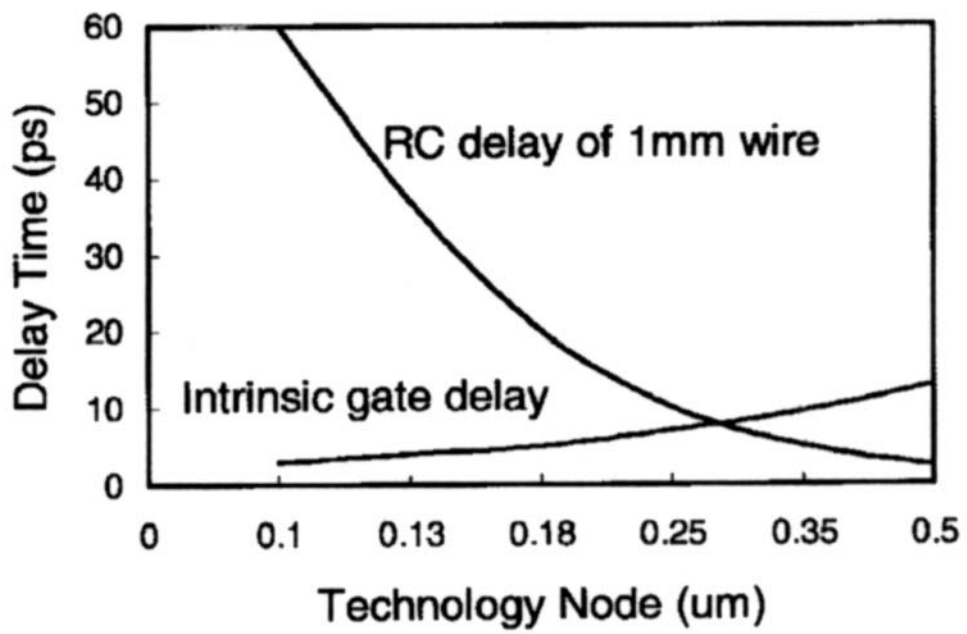


Fig. 1-1 Intrinsic gate delay vs. interconnect RC delay at minimum design rules of each technology node.

Chapter 2

Multi-Chamber Cu CVD System and Cu Precursor

2.1 Multi-Chamber Low Pressure Cu CVD System

A multi-chamber low pressure CVD system with a warm wall reaction chamber built in our laboratory is used for this thesis study. Figure 2-1 shows the schematic diagram of this CVD system, and the photographs of the apparatus are given in Fig. 2-2 and Fig. 2-3. There are four chambers in the CVD systems: (1) loading chamber, (2) transfer chamber, (3) plasma pretreatment chamber, and (4) reaction chamber. Besides these four chambers, the apparatus also contains a precursor delivery system and a catalyst injection system. The details of each chamber and sub-system are described as follows.



(1) Loading Chamber

The loading chamber is a buffer between the controlled vacuum environment inside the CVD system and the atmospheric environment outside the system. The function of this chamber is to handle the substrate input and output. The substrate wafer is placed on an aluminum made substrate holder; either a whole piece of wafer up to an 8-inch diameter or broken pieces of wafer can be placed on the substrate holder. The substrate wafer (together with the substrate holder) can be transferred to any desired chamber via a robot arm that is set in the transfer chamber.

(2) Transfer Chamber

This is a hexagonal shaped chamber directly connected to each of the other chambers of this multi-chamber CVD system. The transfer chamber houses a robot arm, the function of which is to carry the substrate holder and transfer it to the designated chamber. The operation of the robot arm is controlled and monitored by a robot controller via a host computer system. Figure 2-4 is a photograph showing the robot arm in the transfer chamber.

(3) Pre-treatment Chamber

Prior to the deposition of copper films, the substrate wafers can be pre-treated by plasma in this chamber. Figure 2-5 shows the schematic diagram of the pre-treatment chamber. The chamber wall is grounded, and a 600W power generator operated at a radio frequency of 13.56 MHz is used for the plasma generation. The plasma can be induced in the pre-treatment chamber by a negative DC bias [17]. Various gases, including Ar, N₂ and H₂, can be introduced into the chamber for the generation of different plasma [18,19]. The plasma treatment on the substrate surface can be classified into two different types: physical sputtering treatment (such as Ar-plasma) and chemical reaction treatment (e.g. H₂-plasma).

(4) Reaction Chamber

This is the chamber where reaction of precursor takes place to deposit the Cu film. Figure 2-6 shows a schematic diagram of the reaction chamber used for Cu film deposition. On top of the chamber there is a shower-head injector, through which the Cu precursor carried by the carrier gas is introduced into the reaction

chamber. Under the injector there is a substrate holder, which can be heated by a resistive heating element. The substrate holder is rotatable so as to obtain a better uniformity of the deposited film. It can also be moved in vertical direction so that the distance between the injector and the substrate can be adjusted. The side wall of the cylindrical reaction chamber as well as the Cu precursor injector is kept at a temperature of 45°C by a circulating warming water to prevent Cu precipitation. The reaction chamber of this CVD system can be pumped down to a background pressure of 10^{-7} Torr before the deposition process to ensure the contamination free deposition environment.

(5) Direct Liquid Injection (DLI) Delivery System of Precursor

The liquid Cu precursor is delivered by a direct liquid injection (DLI) system, which is composed of a liquid flow meter (LFM) and a controlled evaporation mixer (CEM). A schematic diagram of the DLI system is shown in Fig. 2-7. Initially, the liquid precursor is propelled by the nitrogen gas through the LFM, which can precisely control the mass flow of the liquid precursor. The precursor is then vaporized in the CEM unit and mixed with the carrier gas. Finally, the carrier gas with its carried precursor is directed into the reaction chamber through the gas injector.

(6) Catalyst Storage and Injection System

Liquid C_2H_5I was used in this study to provide iodine (I_2) as catalyst for the CVD of Cu films. C_2H_5I has a high vapor pressure of 137.52mmHg at 25°C. In this study, the container of the liquid C_2H_5I was maintained at a constant temperature of 25°C, and a mass-flow controller (MFC) is connected to the container through a valve, as shown schematically in Fig. 2-8. When the valve is

opened, the iodine containing vapor will enter the reaction chamber by diffusion. The parameters of the mass-flow controller are set ready at the beginning and the vapor flow is totally controlled by the valve.

2.2 Real-time Automatic Monitor and Controller System

Figure 2-9 shows the automatic controlling system of the multi-chamber Cu-CVD system (an automatic remote monitor and controller (ARMC) system). The design concept of this automatic controlling system is focused on the requirements of gas transport, vacuum procedure sequences controlling, substrate plasma treatment, substrate heating control, pressure control, safety protection handling, users friendly interface, and convenient maintenance.

The ARMC system is composed of a host computer, a subsidiary controller, and a unit controller of the Cu CVD apparatus. A communication program is designed to link together the functions of the host computer and the subsidiary controller. Therefore, data and commands can be transferred between them through a dynamic data exchange (DDE) server in Windows98 operation system. In the host computer, a friendly interface program with monitor and control function is operated under the Windows98 operation system, as shown in Fig. 2-10. The deposition process and the procedure sequences are under automatic control by this friendly interface program. What the user needs to do is to program the recipes and process steps correctly and precisely, and the host computer can monitor all of the operation conditions of the Cu CVD system.

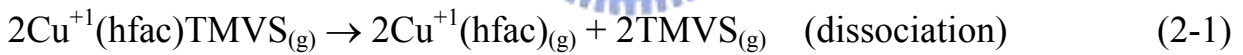
2.3 Reaction of Cu precursor

The Cu precursor used in this thesis study is a liquid Cu(I) precursor of

Cu(1,1,1,5,5,5-hexafluoroacetylacetonate)trimethylvinylsilane [Cu^I(hfac)TMVS] plus 2.4wt%TMVS developed by SCHUMACHER company [11,19]. The 2.4wt%TMVS additive promotes stability of the precursor.

The Cu^I(β-diketonates) is one of the most promising Cu precursors [19]. The group of Cu(I) precursors has a form of Cu^I(β-diketonates)L, where L is a neutral ligand weakly bonded to Cu. Hexafluoroacetylacetonate (hfac) is the most commonly used β-diketonates. The structure of Cu^I(hfac)L is similar to that of Cu^{II}(hfac)₂, with the L ligand replacing one of the hfac rings. Depending on the L ligand, CVD of Cu films may have a selective deposition property. Low resistivity Cu films can be deposited from Cu^I(hfac)TMVS at temperatures below 200°C.

It has been proposed that the complete disproportionation reaction of the Cu^I(hfac)TMVS precursor consists of four steps as follows [20].



where (g) denotes “gas phase” and (s) denotes “adsorbed on substrate surface.” The first step involves the decomposition of Cu(hfac)TMVS into Cu⁺¹(hfac) and TMVS species by the gas phase reaction (Eq. 2-1); this is because Cu-TMVS in the Cu(hfac)TMVS precursor is a weak bond compared to the Cu-hfac bond. This is followed by the adsorption of the Cu⁺¹(hfac) species on the substrate surface

(Eq. 2-2). The $\text{Cu}^{+1}(\text{hfac})$ species then undergo a disproportionation reaction to produce the Cu metal and the Cu(II) species $[\text{Cu}^{+2}(\text{hfac})_2]$ (Eq. 2-3). Finally, the volatile $\text{Cu}^{+2}(\text{hfac})_2$ by-product desorbs from the substrate surface (Eq. 2-4). The reaction step 3 (Eq. 2-3) is the key step of Cu nucleation on the substrate surface, which involves a process of electron exchange between the adsorbed $\text{Cu}^{+1}(\text{hfac})$ and the substrate surface. Thus, it is easier to deposit Cu film on a conducting substrate than on an insulating substrate. The overall disproportionation reaction of Cu film deposition is given by the following equation:

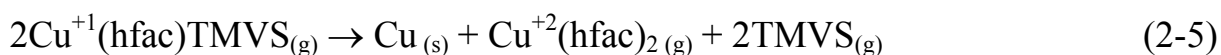


Figure 2-11 illustrates the four steps of Cu film deposition by $\text{Cu}(\text{hfac})\text{TMVS}$ precursor.



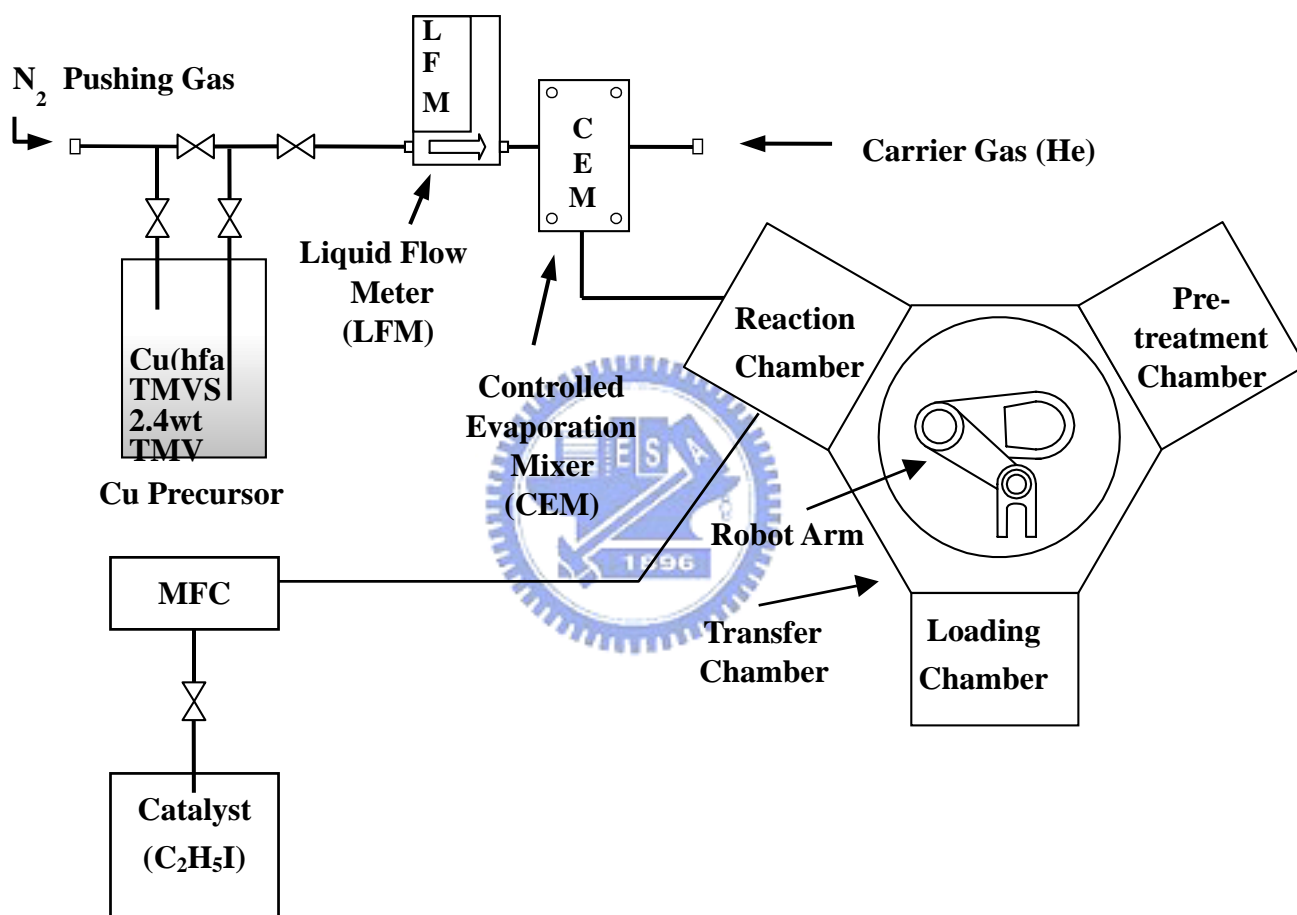


Fig. 2-1 Schematic diagram of the multi-chamber low pressure CVD system used in the study of this thesis.

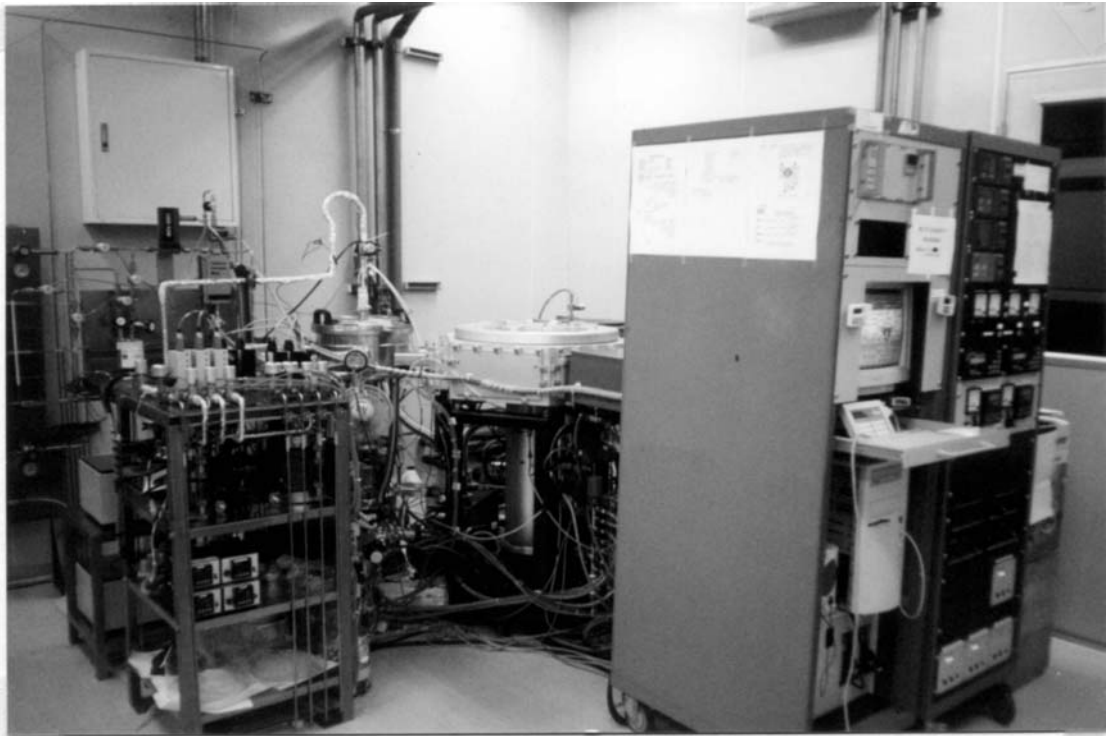


Fig. 2-2 The panorama photograph of the multi-chamber Cu CVD apparatus.

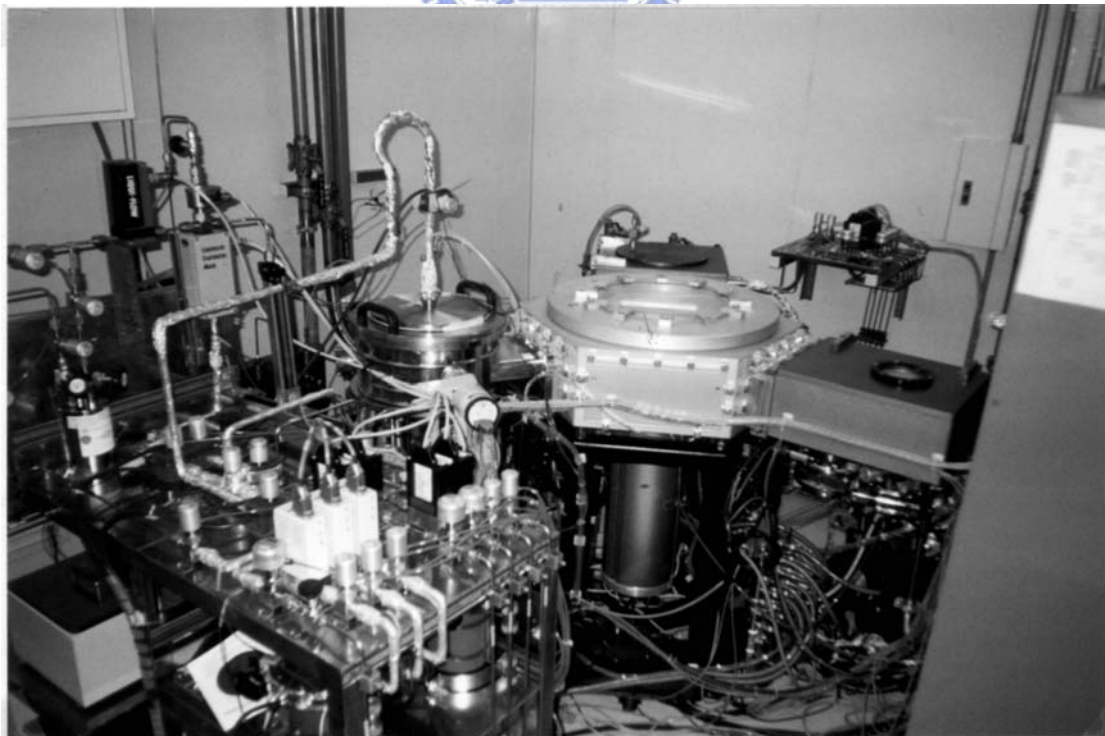


Fig. 2-3 Photograph showing the cluster-chamber, DLI system, and gas piping system.



Fig. 2-4 Photograph showing the robot arm in the transfer chamber.

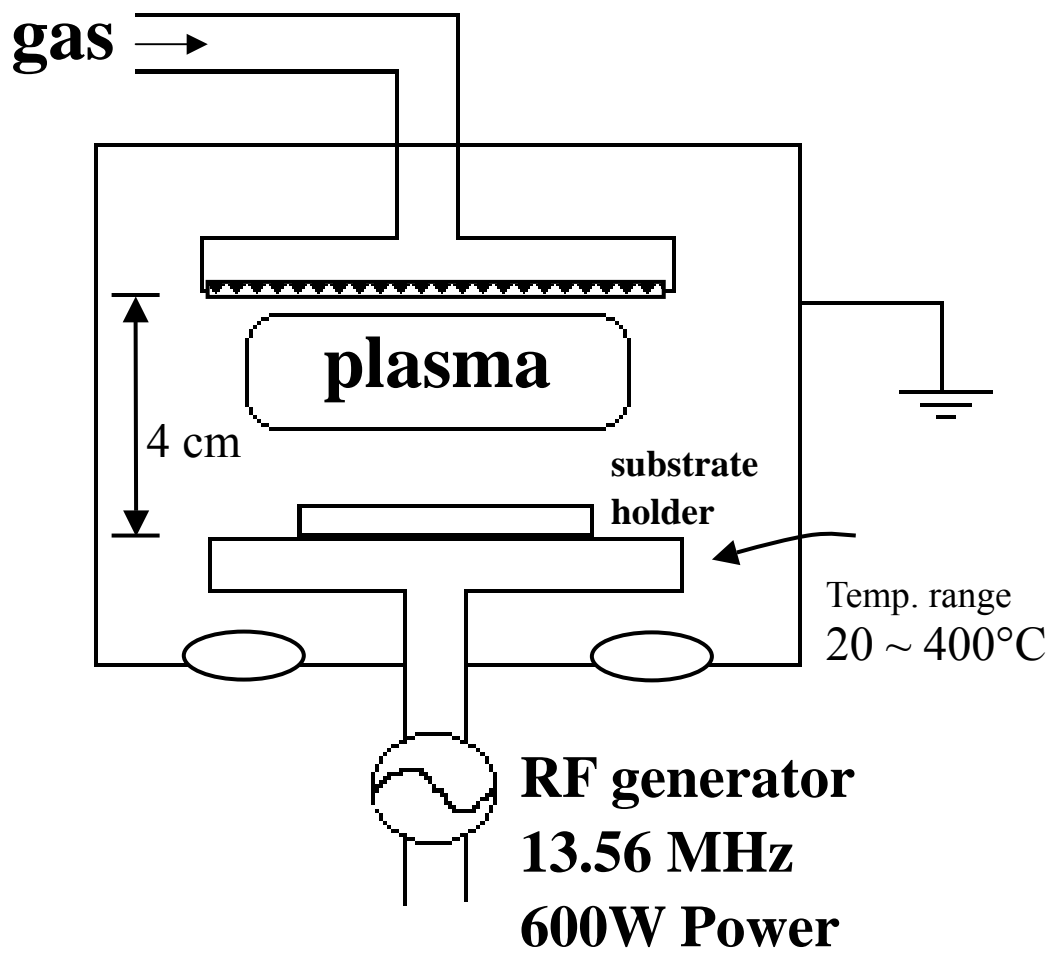


Fig. 2-5 Schematic diagram of the pretreatment chamber.

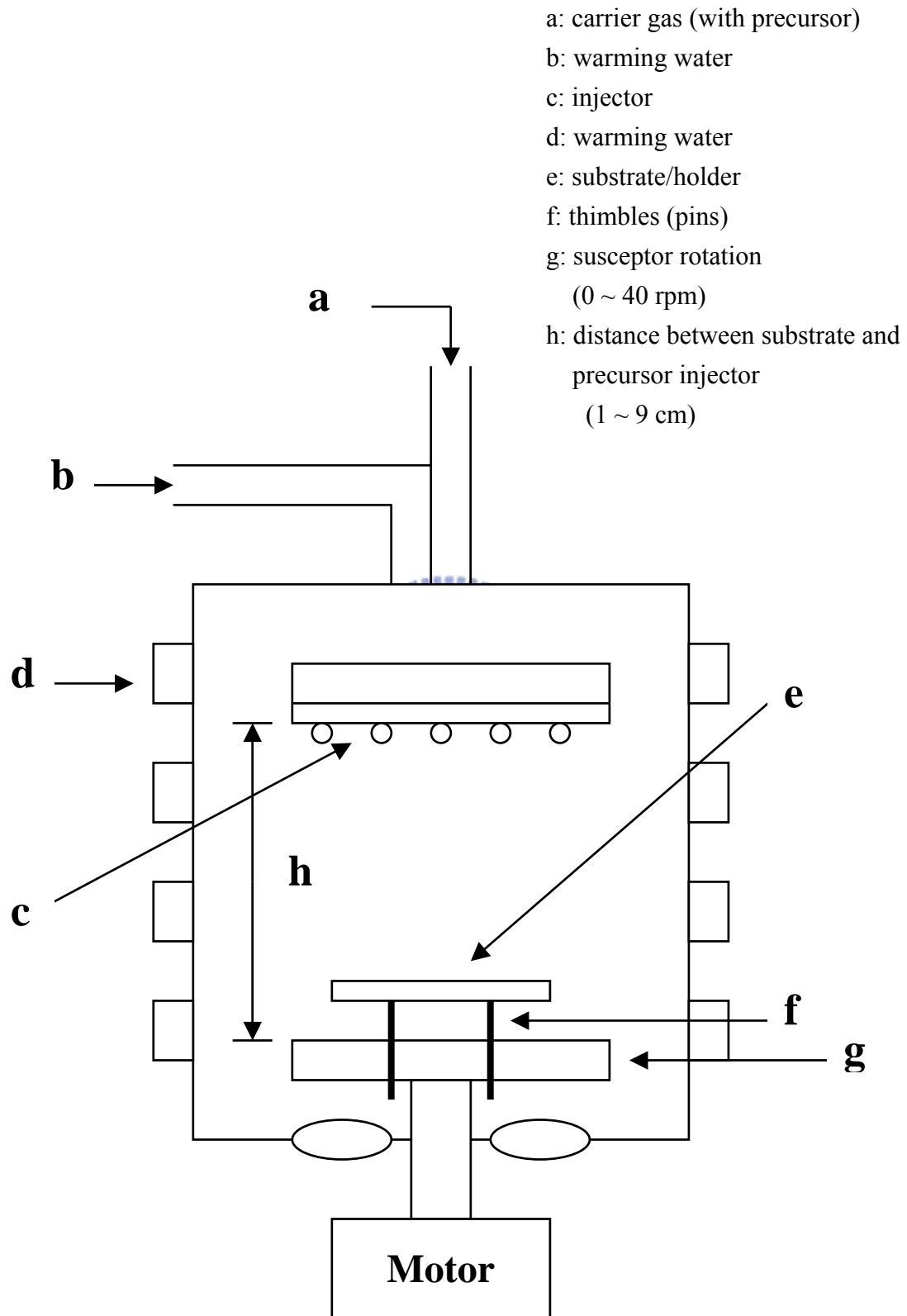


Fig. 2-6 Schematic diagram of the reaction chamber (copper deposition chamber).

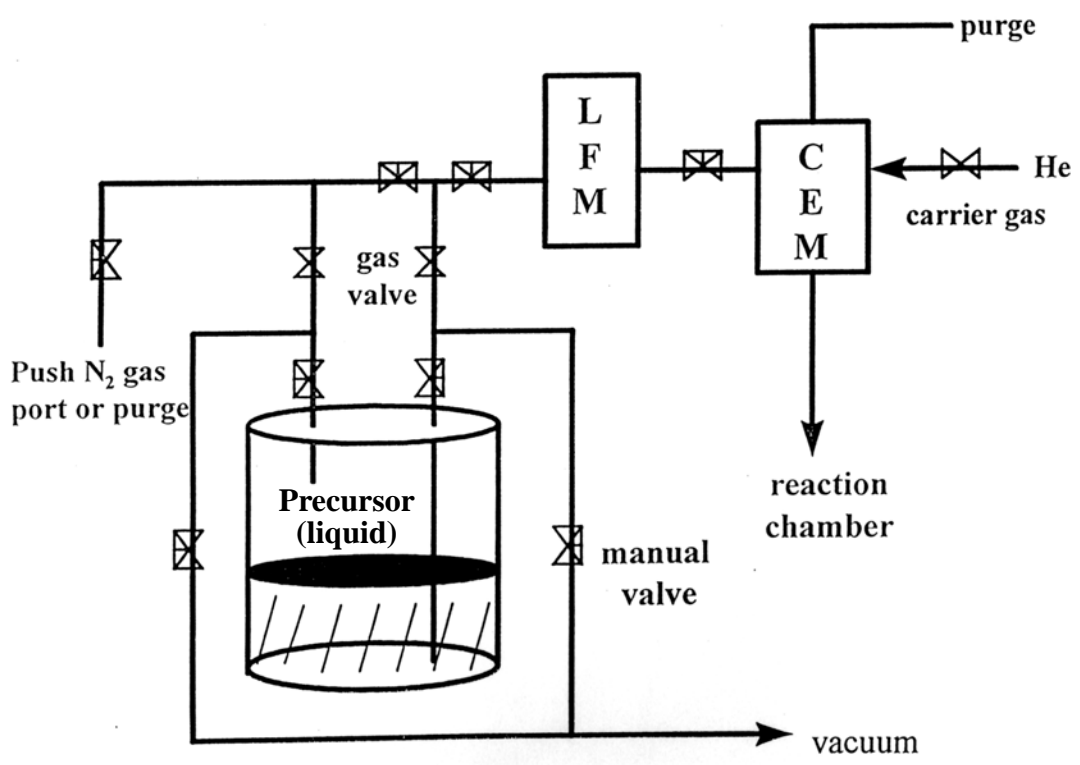


Fig. 2-7 Schematic diagram of the direct liquid injection (DLI) precursor delivery system.

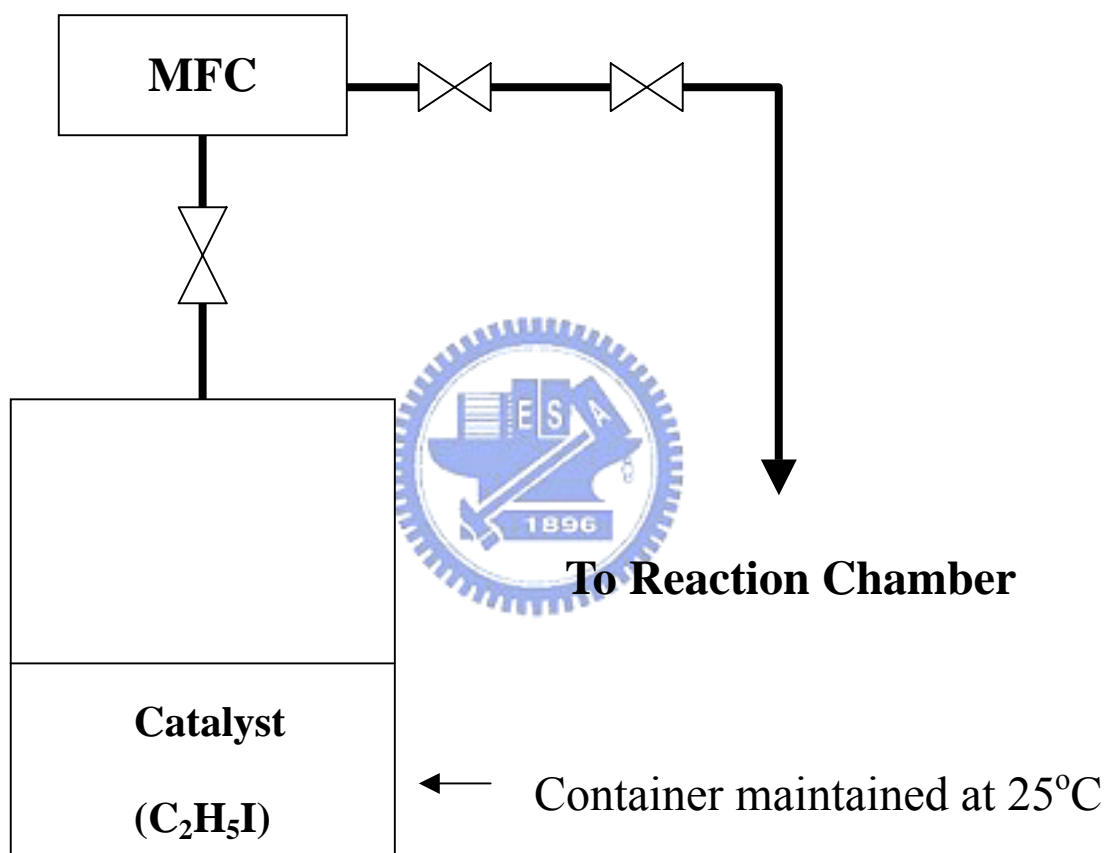
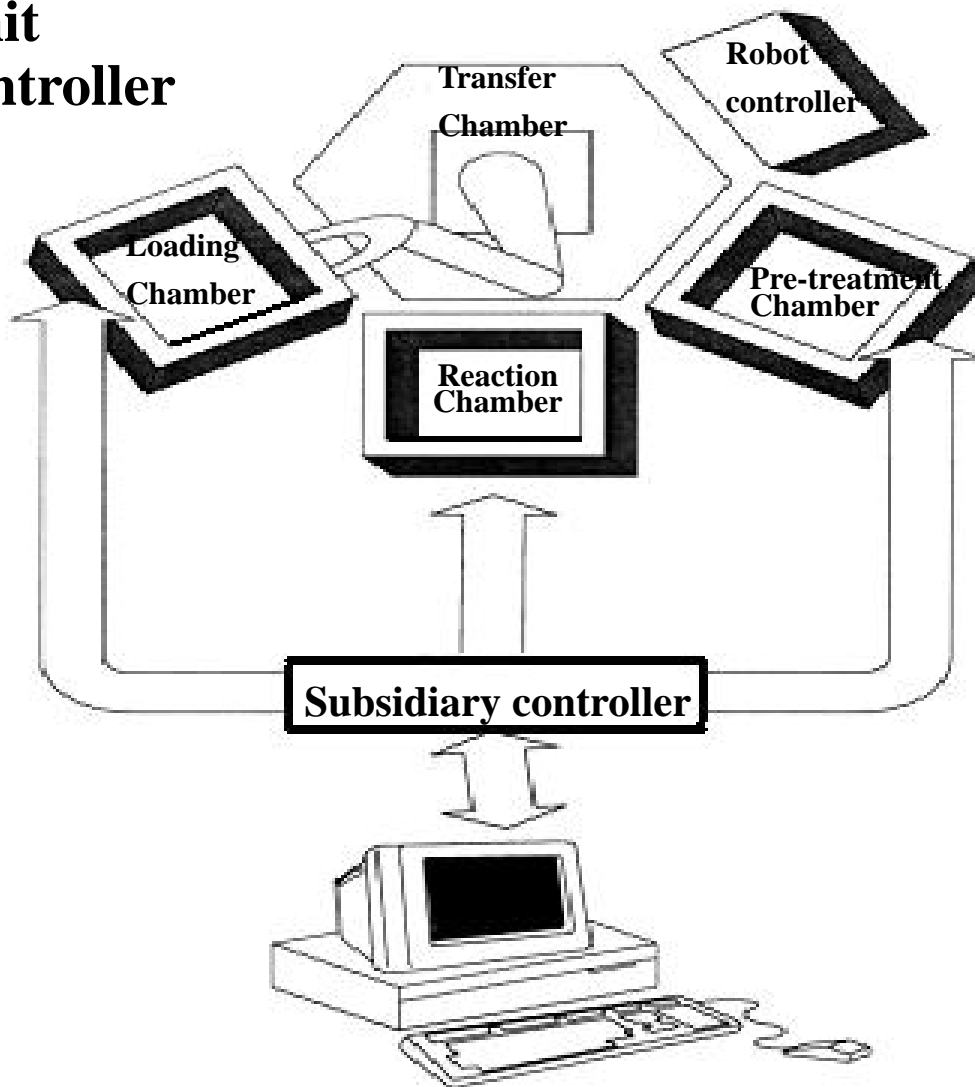


Fig. 2-8 Schematic diagram of the catalyst storage and injection system.

Unit controller



Host Computer

Fig. 2-9 Schematic diagram of the automatic remote monitor and controller (ARMC) system, which is composed of a host computer, a subsidiary controller, and a unit controller of the Cu CVD apparatus.

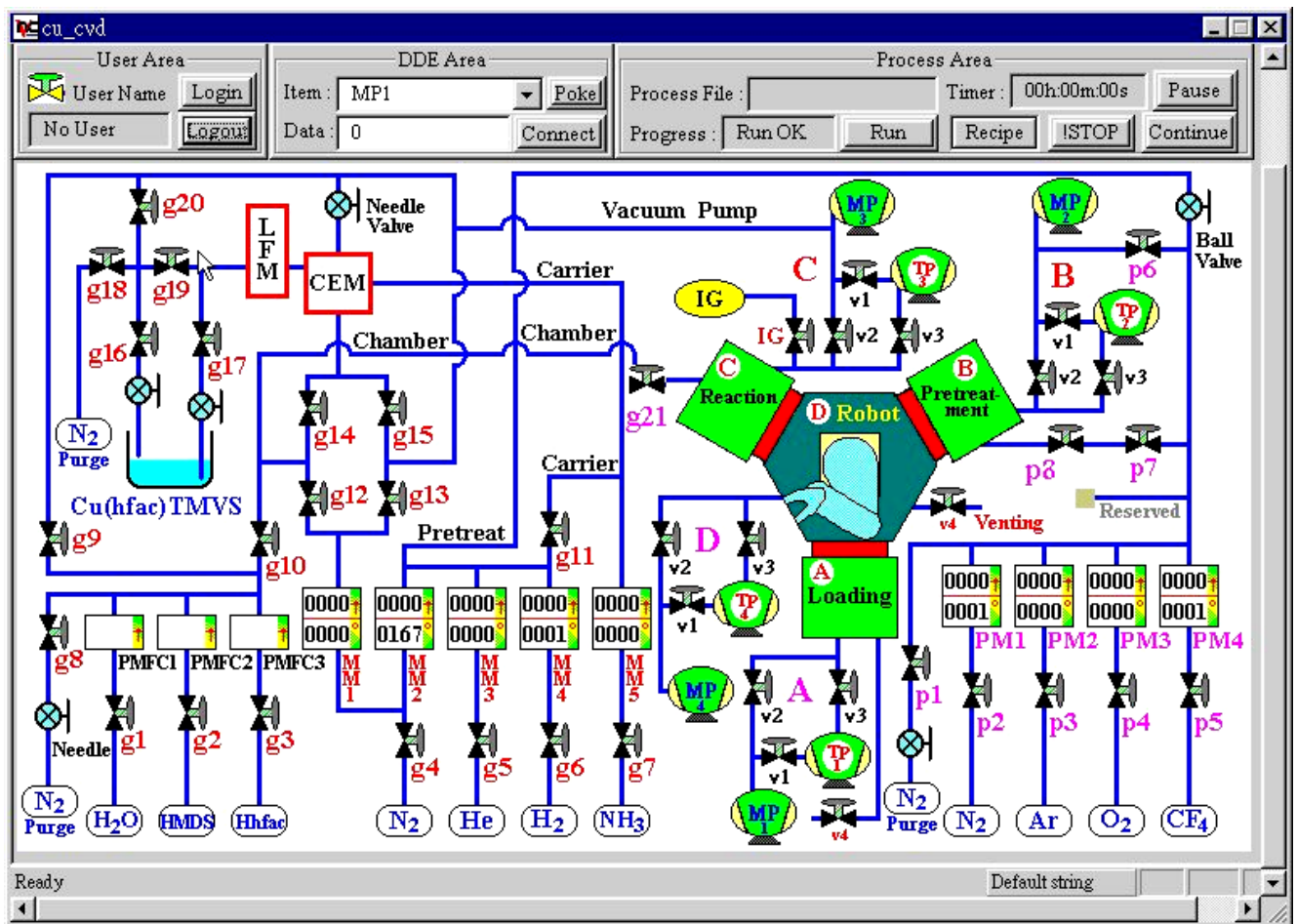


Fig. 2-10 The friendly monitor and control program displays in the host computer screen.

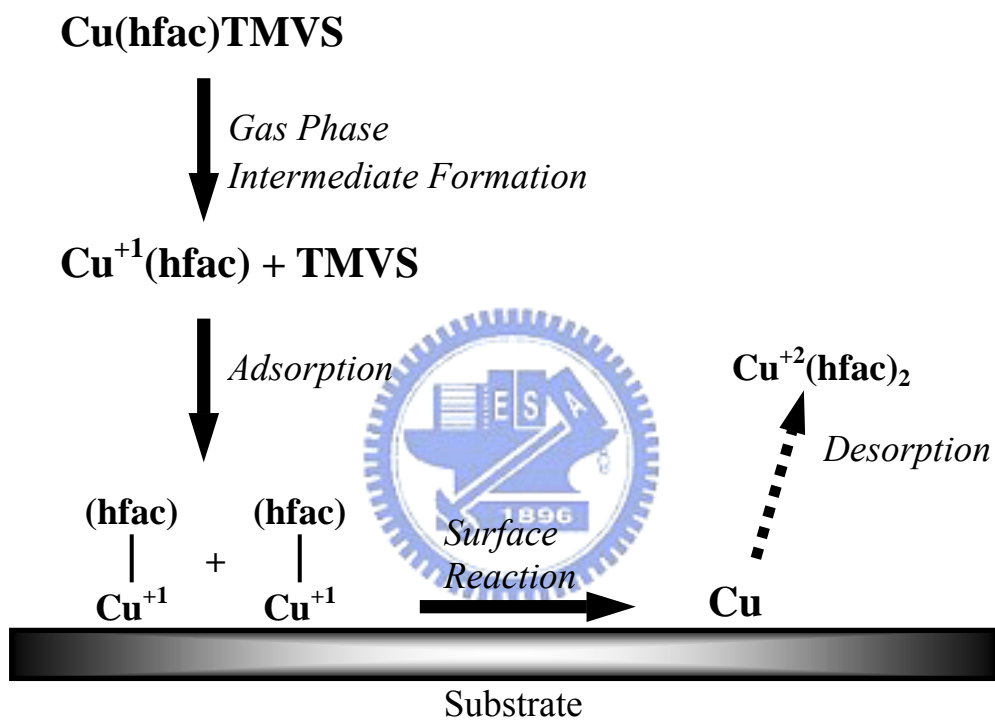


Fig. 2-11 The deposition mechanism of Cu film by Cu(hfac)TMVS precursor.

Chapter 3

Nucleation of Cu Using Iodoethane as Catalyst

3.1 Introduction

When a metal film is deposited by CVD method, the film property is directly affected by the nucleation process, which is very sensitive to the substrate surface condition [21, 22]. In this thesis, iodoethane (C_2H_5I) is used as catalyst for substrate surface treatment prior to the deposition process of Cu films. Effects of iodine adatoms on the nucleation of Cu on TaN substrate are investigated in this chapter by measuring the wetting angle of Cu grains in the nucleation stage of Cu-CVD.



3.2 Experimental Details

The TaN-layer-covered Si wafer was used as the substrate for the nucleation study of Cu-CVD. The TaN layer was deposited to a thickness of 25 nm on a 500-nm-thick thermal SiO_2 -covered Si wafer (TaN(25nm)/ SiO_2 (500nm)/Si). The TaN film was sputter-deposited using a Ta target in an Ar/ N_2 gas mixture; the flow rates of Ar and N_2 were 55 and 2.5 sccm, respectively, for making the gas mixture. The as-deposited TaN film has a resistivity of $288\mu\Omega\text{-cm}$, and the film's composition is $TaN_{0.85}$ as determined by RBS.

The TaN substrate wafer (TaN/ SiO_2 /Si) placed on the substrate holder was loaded into the load-locked chamber of the Cu CVD system. When the pressure of all relevant chambers was pumped down to 2×10^{-6} torr, the substrate wafer was transferred to the reaction chamber via the transfer chamber. Then, helium (He)

was introduced into the reaction chamber and the chamber pressure was maintained at 150 mtorr, while the substrate holder was heated to the deposition temperature of 160°C. It took approximately 70 min for the substrate holder to reach the temperature of 160°C. If the substrate surface is to be treated with catalyst (C_2H_5I was used as catalyst in this study), the reaction chamber was pumped down to 10 mtorr after the substrate holder had reached the desired deposition temperature, and the valve on the pipeline connecting to the catalyst container was opened so that the vaporized C_2H_5I was introduced into the reaction chamber. Then, after the pressure in the reaction chamber had reached 1 torr, the chamber was pumped down again and kept at 150 mtorr until the valve was closed. In this work, the valve opening time was 3 min. Following the close of the valve to stop the inflow of catalyst, the pressure of the reaction chamber was pumped down to 10 mtorr again, and then helium (He) gas was introduced into the chamber. When the chamber pressure was stabilized at 150 mtorr, the valve to the precursor pipeline was opened so that the liquid precursor was propelled by nitrogen gas through the LFC and was then vaporized in the CEM and mixed with the He carrier gas. The precursor-saturated carrier gas was introduced into the reaction chamber through the gas injector to proceed with the Cu CVD process. Table 3-1 summarizes the major parameters and processing conditions for Cu CVD in this study.

3.3 Results and Discussion

The nucleation process of Cu film on the TaN substrate with and without catalyst treatment was investigated by SEM observation on the surface morphology as well as measuring the wetting angle of the Cu grains nucleated on

the substrate surface. Figure 3-1 and Fig. 3-2 illustrate the top view SEM micrographs showing the Cu grain nucleation process on the control (as-deposited) and C₂H₅I-treated TaN substrates, respectively. Hereafter in this thesis, the as-deposited TaN substrate without the C₂H₅I pretreatment is to be designated as control TaN substrate. It can be seen from Fig. 3-1 and Fig. 3-2 that the Cu species from the precursor are more easily adsorbed on the C₂H₅I-treated substrate, leading to a denser distribution of Cu grains. This indicates that iodine adatoms enhanced the chemisorption of Cu-containing adspecies [Cu(hfac)] on the substrate surface. Thus, Cu can be more easily and uniformly nucleated on the C₂H₅I-treated TaN substrate surface, resulting in shorter incubation time and densely and uniformly distributed Cu grains. This behavior directly affects the formation and growth of Cu film. After the Cu-CVD for 3 min, the nucleation of Cu on the C₂H₅I-treated substrate surface had almost developed into a Cu film, whereas on the control substrate surface the Cu grains were still sparsely distributed and also characterized by nonuniform grain size. This is presumably because the subsequent Cu species are much more easily absorbed on the existing Cu grains than the control TaN substrate surface. The nonuniform size of the nucleated Cu grain will presumably affect the Cu film property, especially the film resistivity, because the highly nonuniform size of the nucleated Cu grain may result in voids in the Cu film and rough film surface, leading to higher resistivity. More discussion in this regard is to be given in chapter 4. On the other hand, the denser and more uniform-sized Cu grains on the C₂H₅I-treated TaN substrate resulted in easier merging of the Cu grains to form a continuous Cu film.

The Cu CVD process and the property of CVD Cu films are closely related to the shape of nucleated Cu grains in the nucleation process. Figure 3-3 shows a

schema of nucleated Cu grain as well as the Young's equation and the definition of wetting angle. According to the Young's equation [23], we have

$$\cos \theta = \frac{\sigma_s - \sigma_i}{\sigma_c} \quad (4-1)$$

where θ is the wetting angle of the copper grain, σ_s and σ_c are respectively the substrate surface energy and the Cu grain surface energy, and σ_i is the interfacial energy between the Cu grain and the substrate. The oblique view SEM micrographs in Fig. 3-4 show the Cu grains nucleation at 160°C and 150 mtorr on TaN substrate with and without the C₂H₅I treatment. The wetting angle of the Cu grains on the control TaN substrate was measured to be about 63° while that on the C₂H₅I-treated TaN substrate was about 94°. The increased wetting angle for the nucleated Cu grains on the C₂H₅I-treated substrate indicates that the C₂H₅I treatment resulted in reduced substrate surface energy and/or increased interfacial energy, thus enhancing the Cu film growth in three dimensions and forming less stable (200) orientation [24]. The Cu grains nucleated on the C₂H₅I-treated substrate look like pillars; this is because the Cu grains nucleated on the C₂H₅I-treated TaN substrate have a large wetting angle. Besides, a larger obtuse wetting angle may imply a smaller contact area between the Cu grain and the substrate surface, resulting in degraded film adhesion [25]. In other words, Cu films grown on the C₂H₅I-treated TaN substrate surface may have a degraded adhesion to the substrate, which was confirmed by Scotch tape adhesion test in chapter 4.

3.4 Summary

This chapter investigates the Cu nucleation on the TaN substrate with and without the C_2H_5I catalyst surface treatment. It was found that the C_2H_5I treatment enhanced the chemisorption of Cu-containing adspecies, and thus reduced the incubation time and accelerated the Cu film formation. For the Cu grains nucleated on the C_2H_5I -treated substrate, the wetting angle increased from 63° to 94° , implying that the C_2H_5I -treated substrate has a reduced surface energy and/or increased interfacial energy; this might promote the vertical growth of nucleated Cu grains, degraded the adhesion to substrate, and enhanced (200) orientation packed configuration.



Table 3-1 Major parameters and processing conditions of Cu CVD used in this study.

Cu CVD processing conditions	
Substrate temperature (°C)	160
Operation pressure (mTorr)	150
Cu precursor flow rate (ml/min)	0.4
Carrier gas (He) flow rate (sccm)	25
Substrate holder rotation speed (rpm)	10
Gas-injector/susceptor distance (cm)	2
CEM temperature (°C)	70
Precursor's delivery line temperature (°C)	72
Reactor (reaction chamber) wall temperature (°C)	45
C ₂ H ₅ I storage temperature (°C)	25
Chamber pressure during catalyst treatment (mTorr)	150

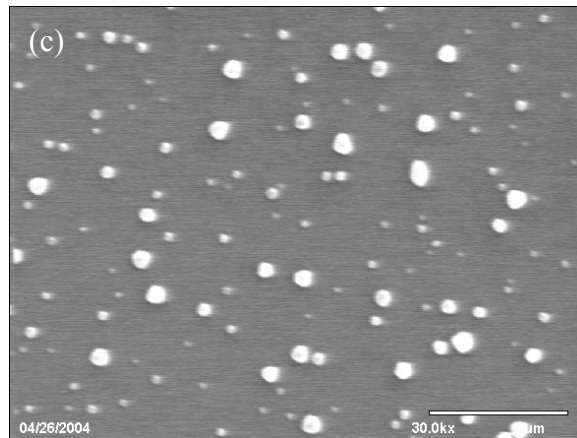
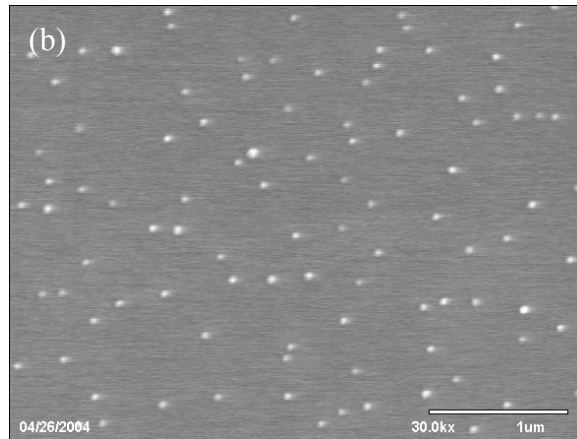
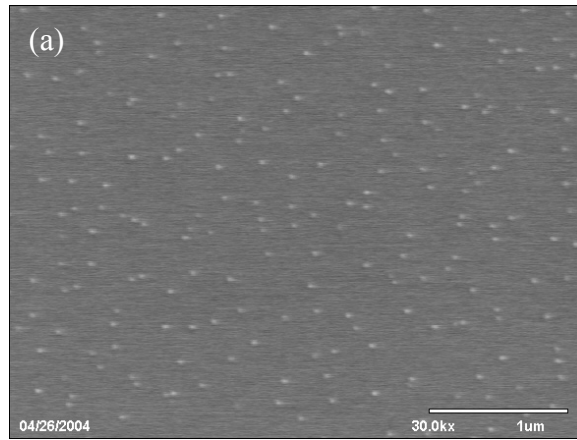


Fig. 3-1 Top view SEM micrographs showing Cu grain nucleation on control TaN substrate

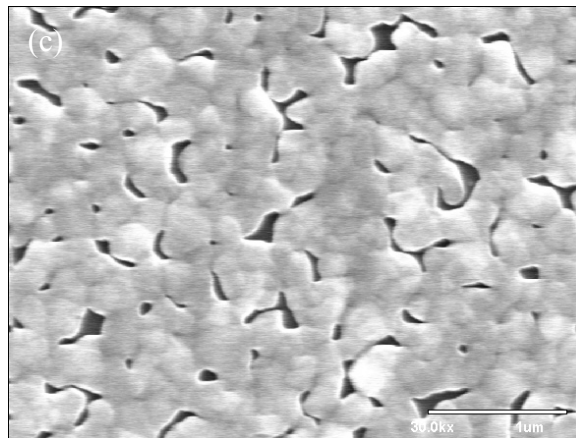
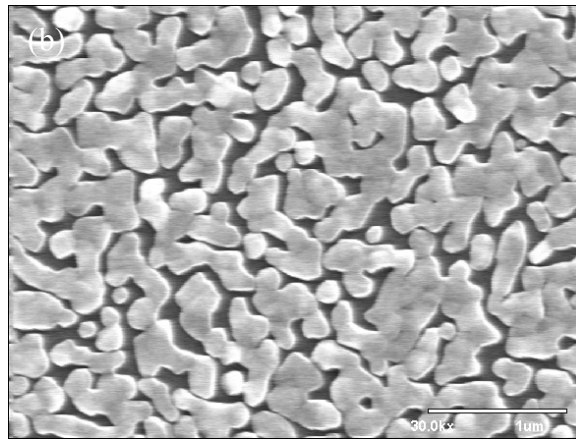
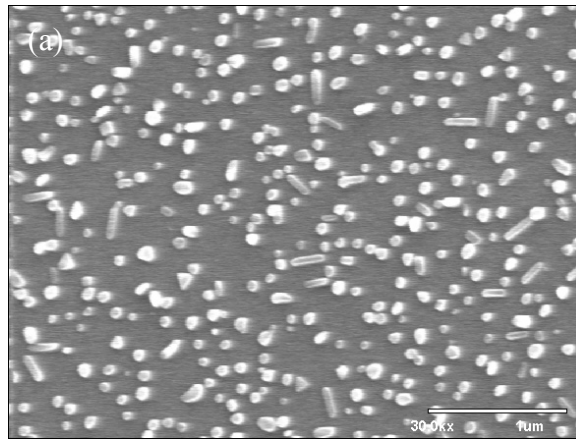
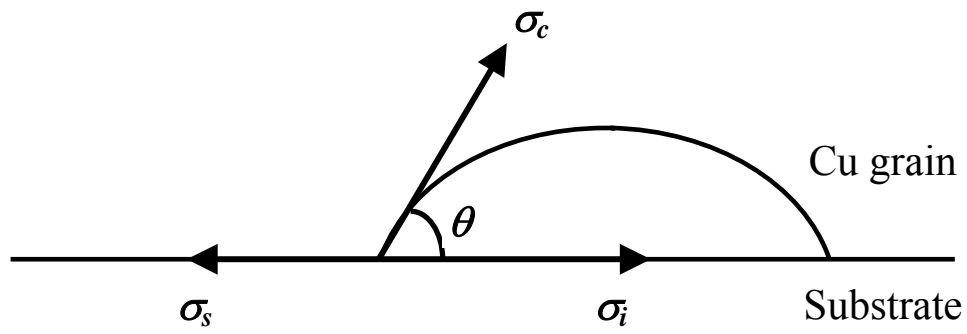


Fig. 3-2 Top view SEM micrographs showing Cu grain nucleation on C_2H_5I -treated TaN substrate for (a) 1 min, (b) 2 min, and (c) 3 min of Cu-CVD.



θ : wetting angle (contact angle)

σ_s : surface energy of substrate

σ_c : surface energy of Cu grain

σ_i : interfacial energy between Cu grain and substrate

$$\cos \theta = \frac{\sigma_s - \sigma_i}{\sigma_c}$$

Fig. 3-3 Schematic illustration of Cu nucleation and Young's equation.

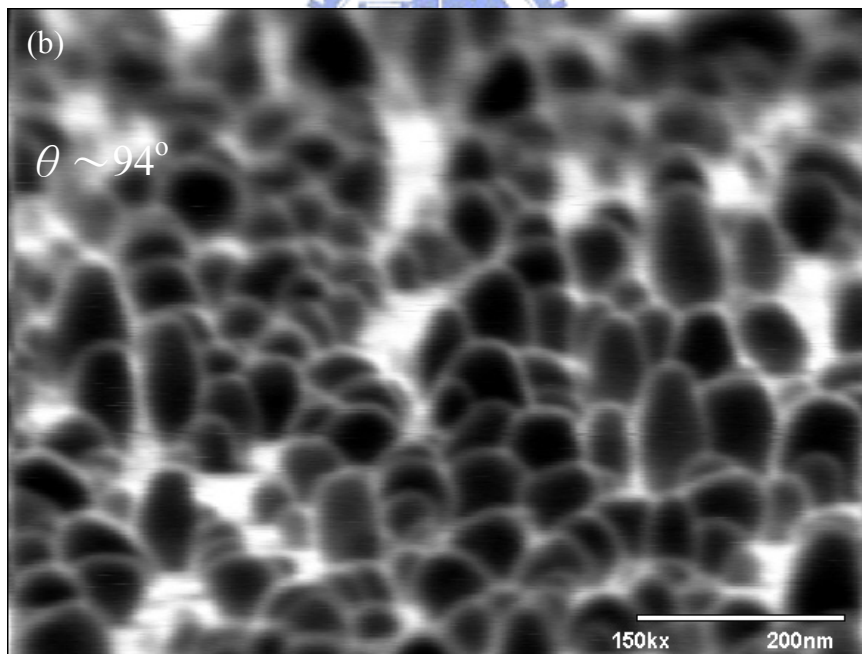
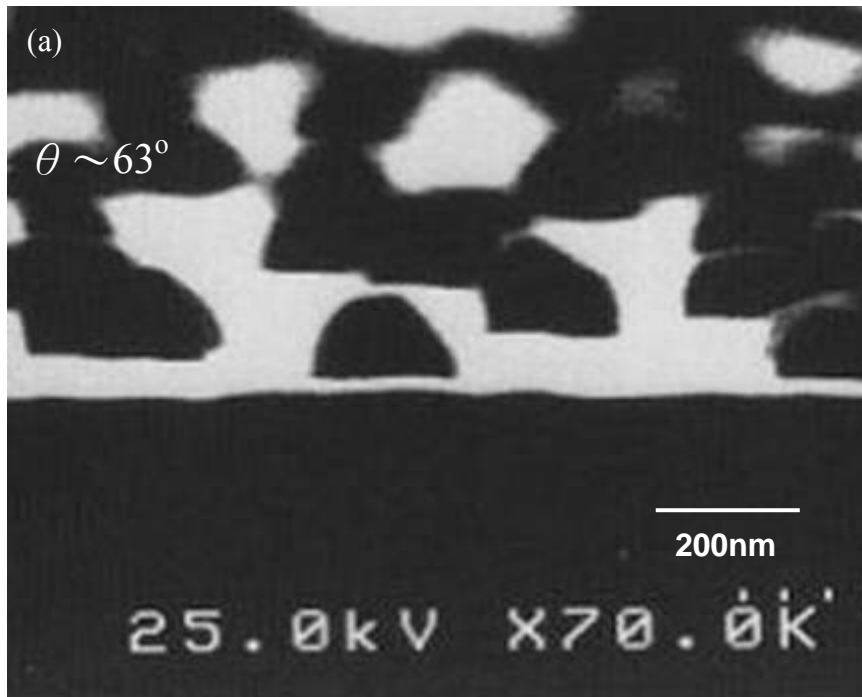


Fig. 3-4 Oblique view SEM micrographs showing Cu grain nucleation for (a) 3 min on as-deposited and (b) 1 min on C_2H_5I -treated TaN substrates.

Chapter 4

CVD Cu Films on C₂H₅I –Treated TaN Substrate

4.1 Introduction

The properties of CVD Cu films are closely related to the initial nucleation of Cu on the substrates [26-28]. Variation of nucleation and growth mechanism of CVD Cu on different substrate conditions leads to different properties of the deposited Cu films. In chapter 3, we have found that C₂H₅I treatment on TaN substrate resulted in different Cu nucleation and film-forming process. In this chapter, properties of Cu films deposited on the C₂H₅I-treated TaN substrate, such as growth rate, surface morphology, film resistivity and film texture, are investigated.



4.2 Experimental Details

CVD Cu films were deposited on the same TaN surface of the substrate wafer TaN(25nm)/SiO₂(500nm)/Si, as was used in the study of chapter 3. The TaN substrate wafer (TaN/SiO₂/Si) placed on the substrate holder was loaded into the load-locked chamber of the Cu CVD system. When the pressure of all relevant chambers was pumped down to 2×10^{-6} torr, the substrate wafer was transferred to the reaction chamber via the transfer chamber. Then, helium (He) gas was introduced into the reaction chamber so as to maintain the chamber pressure at 150 mtorr, while the heating element was turned on to heat the substrate holder to the desired reaction temperature. As the temperature of the substrate holder reached the desired reaction temperature, which usually took

about one hour, the reaction chamber was pumped down to 10 mtorr. Then, the control valve to the catalyst container was opened to guide the vapor phase catalyst of C_2H_5I into the reaction chamber. As the chamber pressure rose to 1 torr in a short time, it was pumped down again and maintained at 150 mtorr until the valve was closed to turn off the catalyst supply. In this study for the effect of catalyst, the control valve to the catalyst container was opened for 3 min. Then, the chamber pressure was pumped down to 10 mtorr again, and He gas was introduced into the chamber. When the chamber pressure was stabilized at 150 mtorr, the control valve to the Cu precursor was opened, and the liquid precursor was propelled by the pushing nitrogen gas through the LFM. It was then vaporized in the CEM and mixed with the He carrier gas. The precursor-saturated carrier gas was introduced into the reaction chamber through the gas injector to proceed with the Cu CVD. In this study, Cu CVD was usually conducted for 10 min. The general processing conditions of Cu CVD for the study in this chapter are the same as those used in chapter 3, as shown in Table 3-1.

The thickness of Cu films was measured using a DekTek profiler and was further verified by cross-sectional scanning electron microscopy (SEM). SEM was also used to observe the surface morphology of the Cu films. A four-point probe was employed to measure the sheet resistance. The X-ray diffraction (XRD) analysis was used for phase identification. The surface roughness of the Cu films deposited was evaluated using atomic force microscopy (AFM).

4.3 Effect of TaN Substrate Treatment by C_2H_5I on CVD Cu Films

Figure 4-1 shows the effective deposition rate of Cu films on the TaN substrate with and without C_2H_5I treatment as a function of substrate temperature

(Arrhenius plot). The effective deposition rate was determined using the thickness of Cu films deposited in a duration of 10 min. Apparently the C₂H₅I treatment on TaN substrate resulted in increase of the effective deposition rate as well as the activation energy. This is presumably due to the shorter incubation time and the much easier nucleation of Cu on the C₂H₅I-treated TaN substrate. Iodine atoms on the TaN substrate promote the dissociation of Cu species in the precursor and accelerate the reaction, resulting in the faster growth rate. The larger wetting angle of Cu grains nucleated on the C₂H₅I-treated TaN substrate, as shown in chapter 3, promotes the three-dimensional growth of Cu grains; this might also be a factor of faster Cu film growth rate. At temperatures above 180°C, the Cu film deposited on the C₂H₅I-treated TaN substrate turned out to be porous, nonuniform, and poorly adhesive that the film easily peeled off. Figure 4-2 illustrates the SEM micrograph for the Cu film deposited on the C₂H₅I-treated TaN substrate at 200°C, showing the nonuniform grain size and the plenty of voids in the Cu film. Figure 4-3 shows the resistivity of Cu films as a function of deposition temperature. The film resistivity is closely related to the impurity content and the film's microstructure [29, 30]. For the films on the control TaN substrate, the slightly higher resistivity at temperatures below 160°C is presumably due to higher contamination of residual impurities from the reaction by-products, while the higher resistivity at temperatures above 160°C is presumably also due to higher contamination of impurities in the film in addition to the porous film structure [30]. The Cu films deposited on the C₂H₅I-treated TaN substrate exhibited lower film resistivity than those deposited on the control TaN substrate, presumably because the iodine atoms on the C₂H₅I-treated substrate weakened the [Cu⁺-(hfac)⁻] ionic bond, promoting and accelerating the dissociation of the [Cu(hfac)] species that is adsorbed on the substrate surface

[13], thus the residual impurities from the reaction by-products had enough time to be pumped away from the film surface. Figure 4-4 and Fig. 4-5 illustrate the SEM micrographs showing the surface morphology of Cu films deposited on the control and C₂H₅I-treated TaN substrates, respectively. On the control substrate, although the Cu films deposited at higher temperatures generally have a larger grain size, they also contain larger voids and the grains appear to be loosely connected. On the other hand, it appears that the Cu films deposited on the C₂H₅I-treated substrate contain fewer voids in comparison with the corresponding Cu films deposited on the control substrate.

Figure 4-6 and Fig. 4-7 show the XRD spectra for the Cu films deposited on the control and C₂H₅I-treated TaN substrates, respectively, at various temperatures. Apparently, C₂H₅I-treatment on TaN substrate had an adverse effect on the growth of Cu film in (111) orientation, in particular at low deposition temperatures. Nonetheless, higher temperatures tended to promote the growth of (111) texture, either on the control or the C₂H₅I-treated TaN substrate.

Figure 4-8 and Fig 4-9 show the AFM images for the Cu films deposited on the control and C₂H₅I-treated TaN substrate, respectively. The RMS roughness of the Cu films deposited in a duration of 10 min on the C₂H₅I-treated TaN substrate is comparable with that deposited on the control TaN substrate. However, it should be noted that the thicknesses of the Cu films are widely different, although they were all deposited in a duration of 10 min.

The adhesion of Cu film to the underlayer substrate was evaluated by a simple Scotch tape pulling test. Table 4-1 shows the results of the test for the adhesion of Cu films to the TaN substrate with and without C₂H₅I treatment. The testing results for the samples of Cu film deposited on C₂H₅I-treated TaN substrate followed by thermal annealing at 400°C for 30 min in N₂ ambient, are

also included in the table for comparison. For the Cu films deposited at and above 160°C on the control TaN substrate, they all passed the Scotch tape pulling test. However, the Cu films deposited on the C₂H₅I-treated TaN substrate all failed to pass the test. The large wetting angle of the nucleated Cu grains on the C₂H₅I-treated TaN substrate at the nucleation stage, because of the reduced substrate surface energy, might be responsible for the degraded adhesion. However, thermal annealing (at 400°C) resulted in slight improvement on the adhesion, although the improvement was not adequate to meet the requirement of practical applications.

4.4 Effect of Post-Deposition Thermal Annealing

Cu films deposited on the TaN substrates with/without C₂H₅I treatment were thermally annealed at 400°C for 30 min in N₂ ambient. It was found that the thermal annealing resulted in the decrease of film resistivity, as shown in Table 4-2, and a slight improvement on the adhesion of Cu film to the C₂H₅I-treated TaN substrate, as shown in Table 4-1. Figure 4-10 and Fig. 4-11 show, respectively, the surface morphology of 400°C-annealed Cu films deposited on the control and C₂H₅I-treated TaN substrates at various temperatures. Compared with Fig. 4-4 and Fig. 4-5, which show the surface morphology of the as-deposited Cu films, it can be seen that the thermal annealing at 400°C resulted in obvious change in surface morphology for all Cu films except the one deposited at 240°C [Fig. 4-10 (f)], which was deposited in the flow-rate-controlled regime. The annealed Cu films exhibited milky or fluid-like surface, showing better connected Cu grains, diminished voids and smoother surface. The AFM images shown in Fig. 4-12 and Fig. 4-13 confirm the smoother

surface of the annealed Cu films. Figure 4-14 shows the improvement of the surface roughness, defined as the percentage decrease of RMS value.

$$\Delta R(\%) = \frac{R_a - R_t}{R_a} \times 100 \%$$

where $\Delta R(\%)$ is the percentage decrease of RMS, and R_a and R_t are the RMS of the as-deposited and 400°C-annealed Cu films, respectively. Figure 4-15 and Fig. 4-16 illustrate, respectively, the XRD spectra for the 400°C-annealed Cu films deposited on the control and C₂H₅I-treated TaN substrates at different temperatures. No obvious change in the XRD intensity peak ratio of Cu(111) to Cu(200) reflections was detected in comparison with that of the as-deposited Cu film (Fig.4-6 and Fig. 4-7).

4.5 Summary

This chapter explores the effects of TaN substrate pretreatment by C₂H₅I catalyst on the CVD-Cu films as well as the effect of post-deposition thermal annealing of Cu/TaN samples. The Cu film deposited on the C₂H₅I-treated TaN substrate exhibited higher deposition rate and lower electrical resistivity in comparison with that deposited on the control TaN substrate, presumably because the iodine atoms on the C₂H₅I-treated substrate surface promoted the dissociation of Cu species. However, it also enhanced the growth of (200) oriented texture and degraded the adhesion of the deposited Cu films to the TaN substrate. Thermal annealing at 400°C resulted in obvious change of the surface morphology as well as reduced surface roughness. Moreover, thermal annealing also resulted in reduced film resistivity and slightly improved Cu film adhesion to C₂H₅I-treated TaN substrate.

Table 4-1 Results of Scotch tape pulling test on the adhesion of CVD Cu films to TaN substrate.

Substrate	Deposition Temperature of Cu Film (°C)					
	140	160	180	200	220	240
Control TaN	F*	P	P	P	P	P
C ₂ H ₅ I-treated TaN	F	F	F			
C ₂ H ₅ I-treated TaN (after 400°C anneal)	F*	F*	F*			

P: Cu film passed the Scotch tape pulling test.

F: Cu film peeled off after Scotch tape pulling test.

F*: Cu film partially peeled off after Scotch tape pulling test.

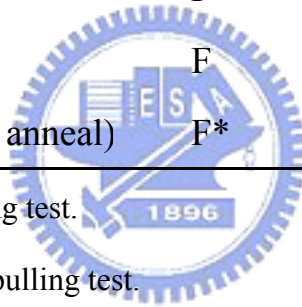


Table 4-2 Effect of thermal annealing (400°C in N₂ for 30 min) on resistivity for Cu films deposited on TaN substrates with/without C₂H₅I treatment.

Deposition temperature (°C)	Resistivity (μΩ-cm)			
	Control substrate		C ₂ H ₅ I-treated substrate	
	as-deposited	annealed	as-deposited	annealed
140	3.35	3.07	1.95	1.90
160	2.26	2.08	2.30	2.25
180	2.77	2.44	2.37	2.27
200	3.24	2.94		
220	3.50	3.07		
240	7.83	7.44		

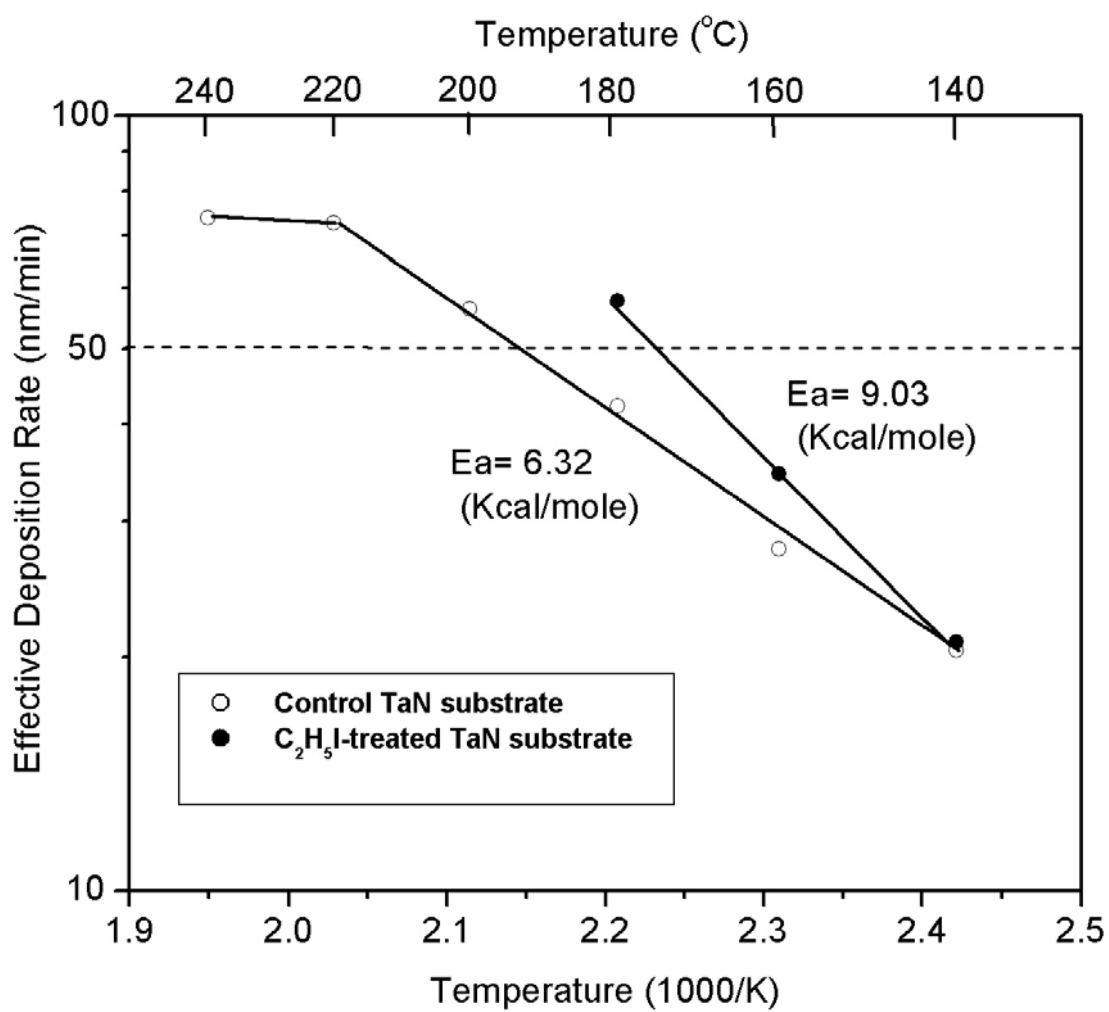


Fig. 4-1 Effective deposition rate vs. substrate temperature (Arrhenius plot) for Cu films deposited at a pressure of 150 mtorr on TaN substrate with and without C₂H₅I treatment.

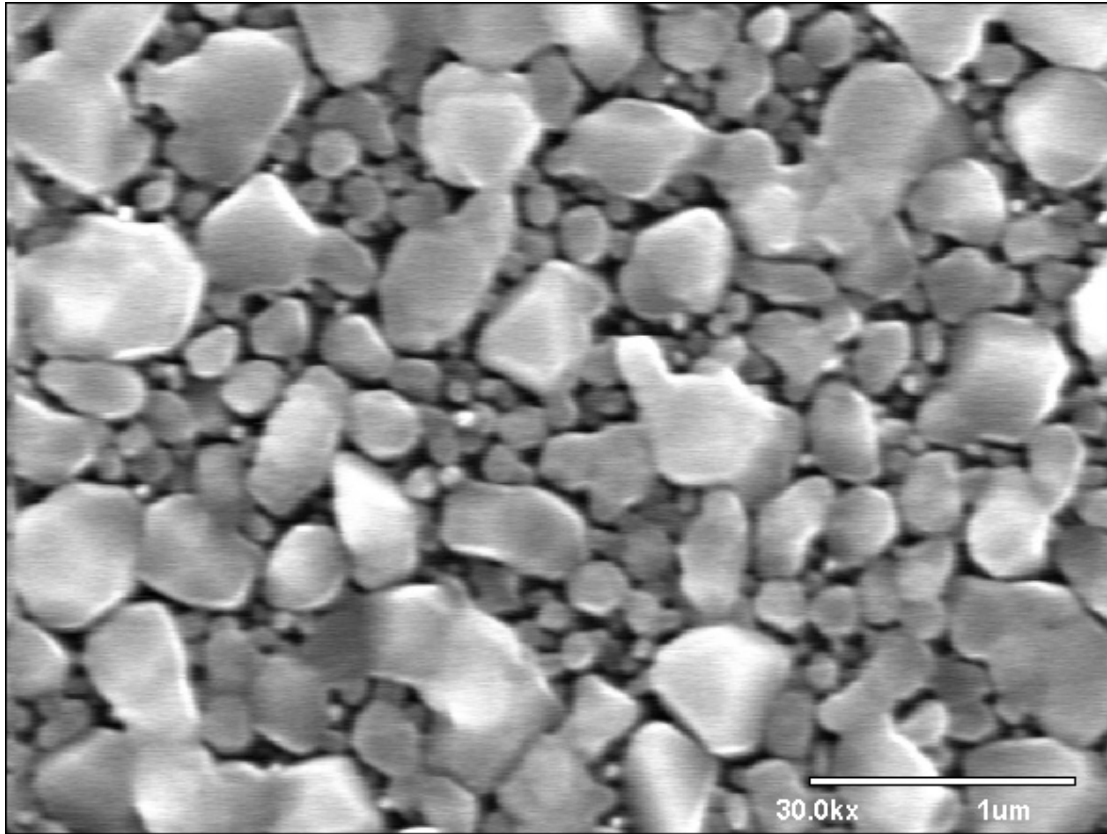


Fig. 4-2 SEM micrograph showing surface morphology of Cu film deposited on C_2H_5I -treated TaN substrate at $200^\circ C$.

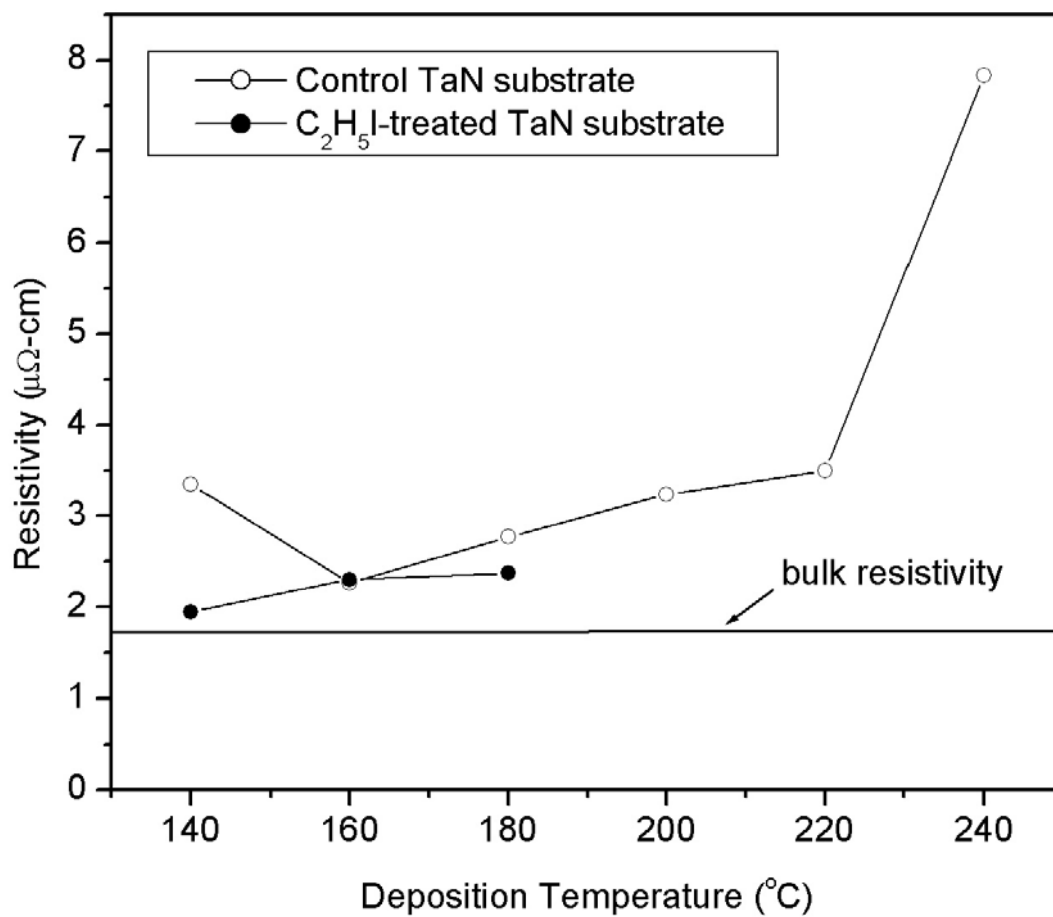


Fig. 4-3 Resistivity vs. deposition temperature for Cu films deposited at a pressure of 150 mtorr on TaN substrate with and without $\text{C}_2\text{H}_5\text{I}$ treatment.

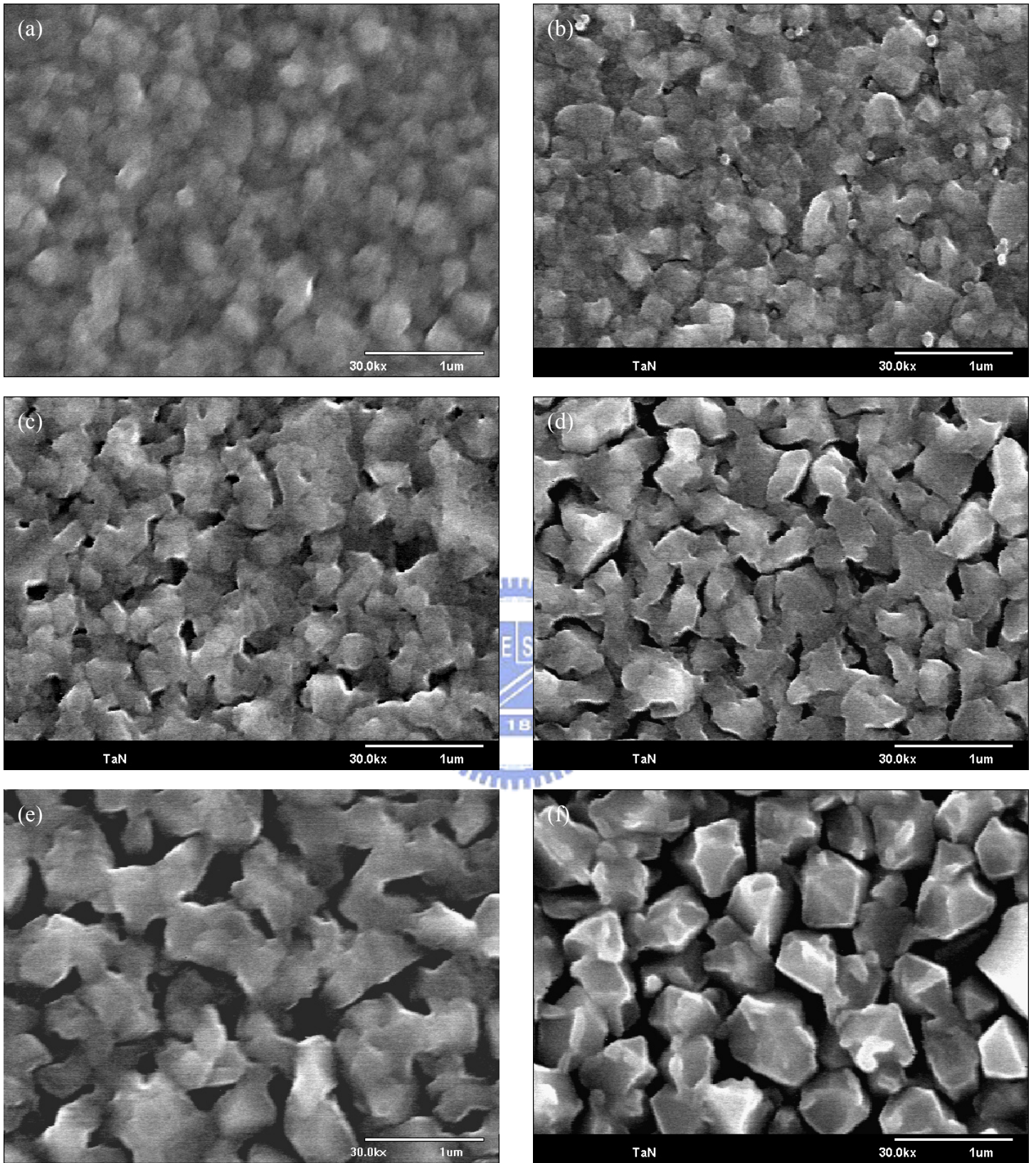


Fig. 4-4 SEM micrographs showing surface morphology of Cu films deposited on control TaN substrate at (a) 140°C, (b) 160°C, (c) 180°C, (d) 200°C, (e) 220°C, and (f) 240°C.

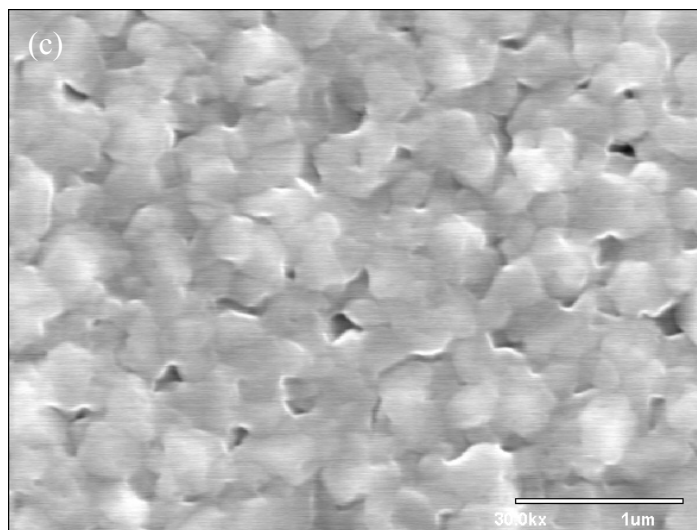
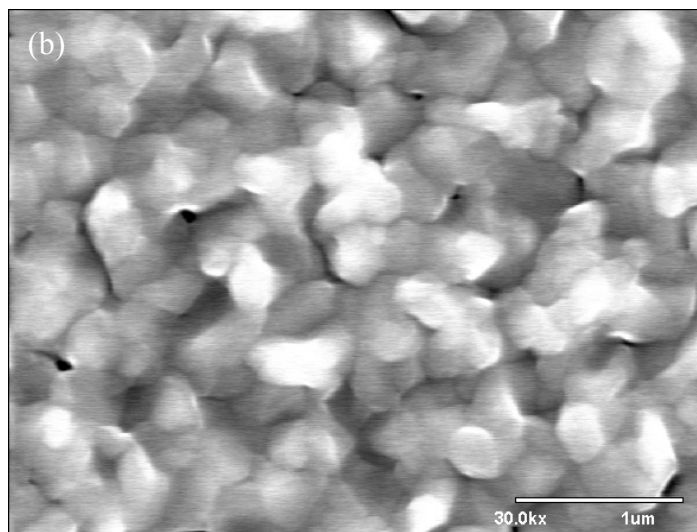
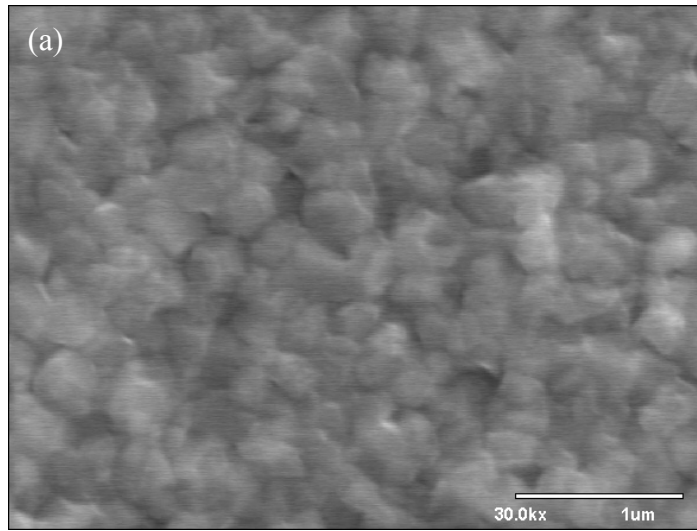


Fig. 4-5 SEM micrographs showing surface morphology of Cu films deposited on C_2H_5I -treated TaN substrate at (a) $140^{\circ}C$, (b) $160^{\circ}C$, and (c) $180^{\circ}C$.

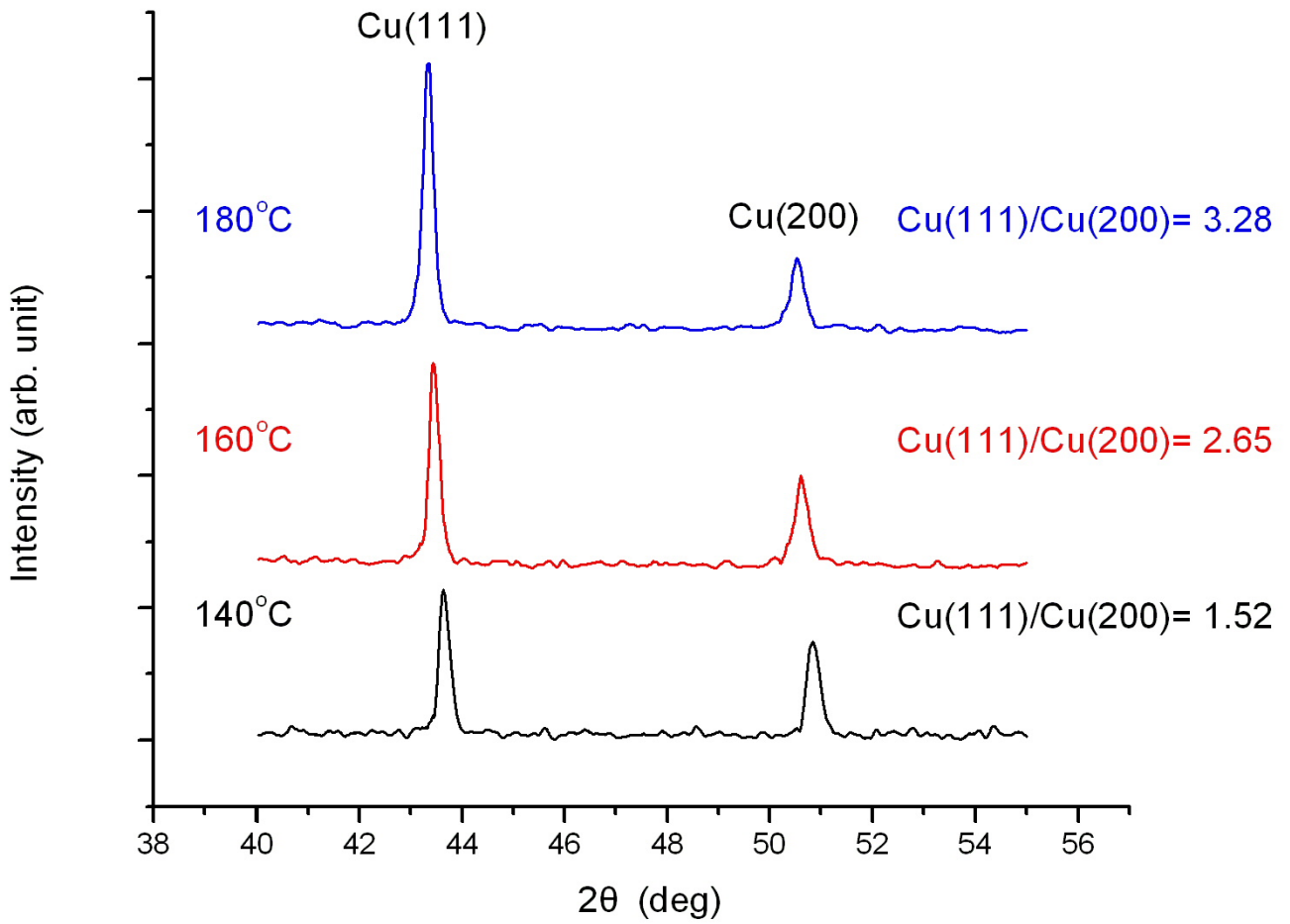


Fig. 4-6 XRD spectra of Cu films deposited on control TaN substrate at different temperatures.

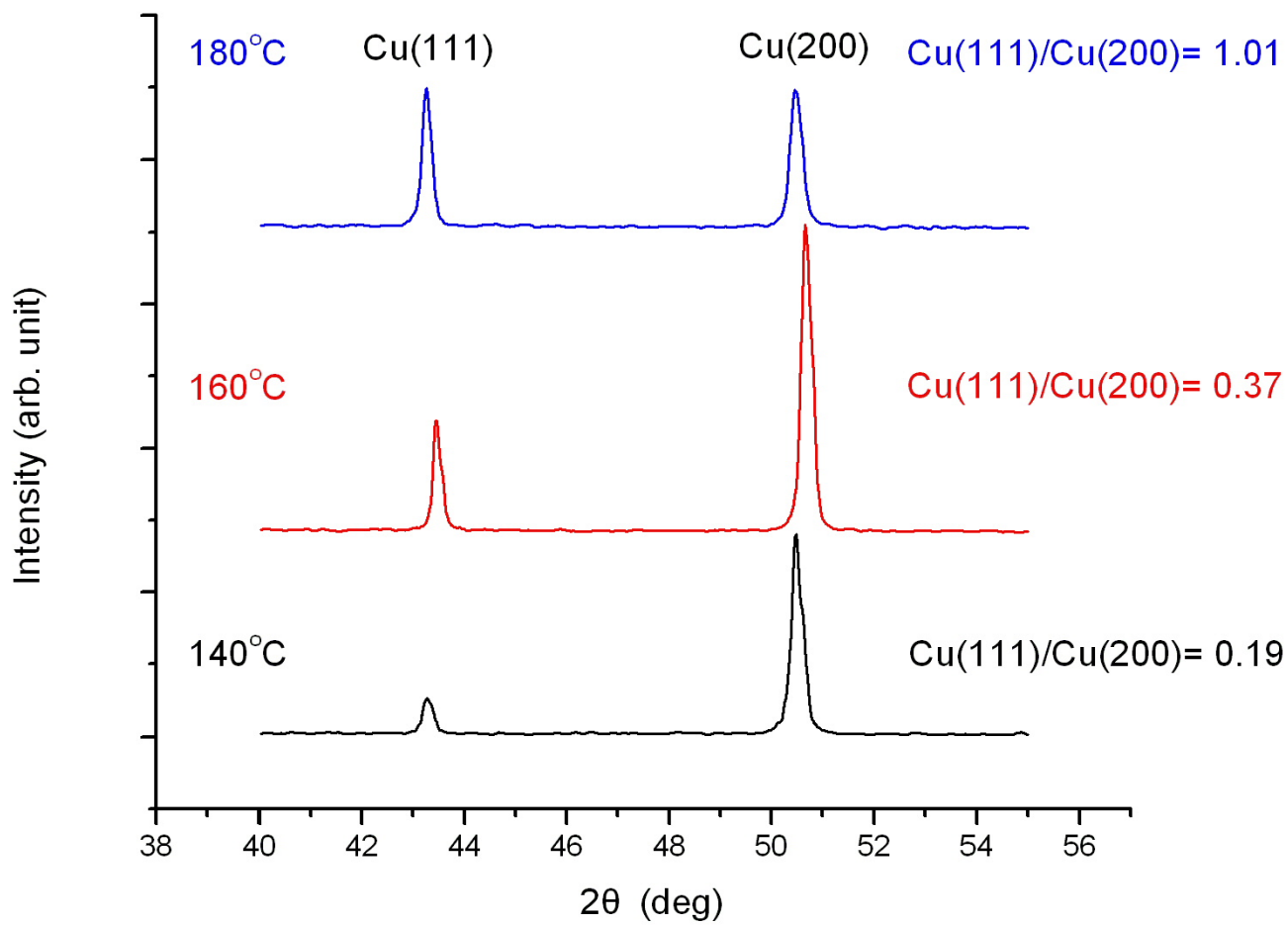
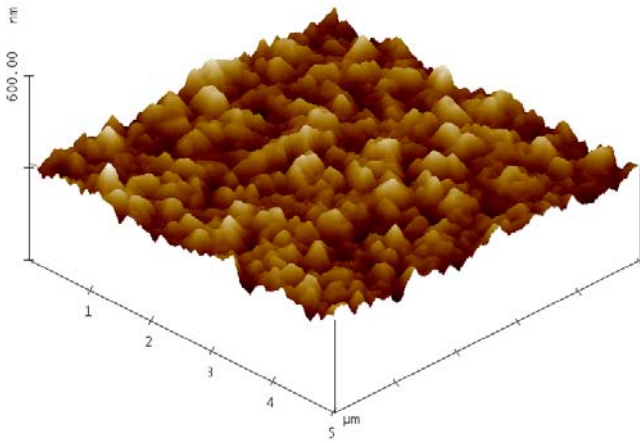


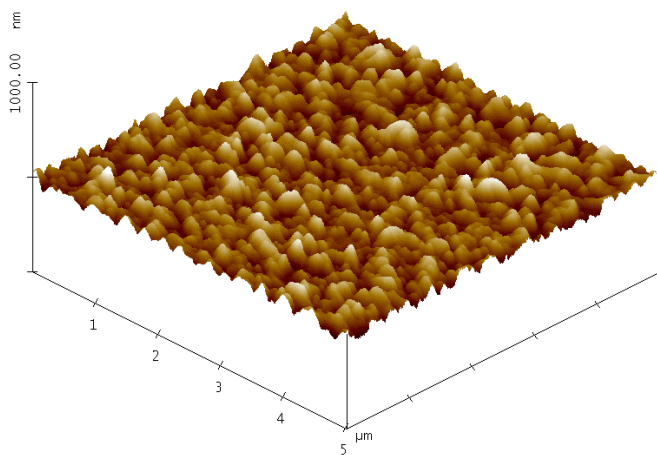
Fig. 4-7 XRD spectra of Cu films deposited on C₂H₅I-treated TaN substrate at different temperatures.



@ 140°C

RMS = 19.599nm

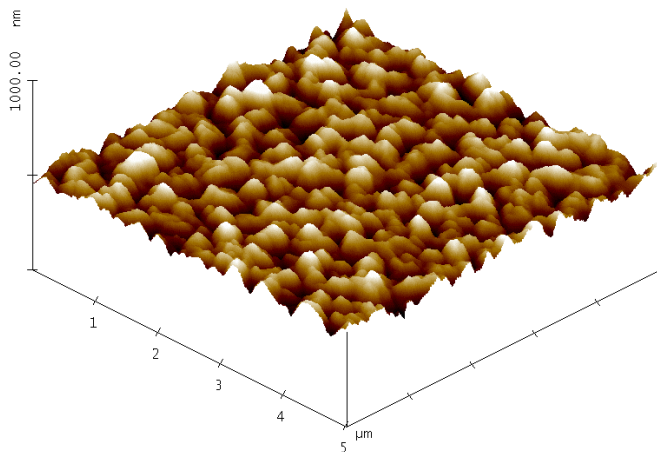
Thickness = 207nm



@ 160°C

RMS = 23.670nm

Thickness = 276nm



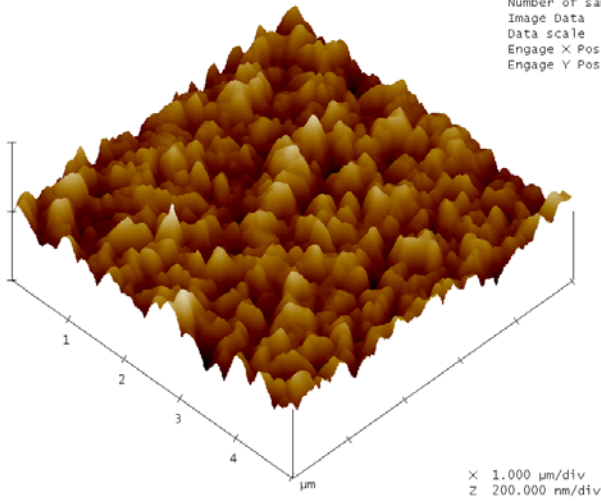
@ 180°C

RMS = 30.746nm

Thickness = 422nm

Fig. 4-8 AFM image showing surface roughness for Cu films deposited in a duration of 10 min on control TaN substrate at different temperatures.

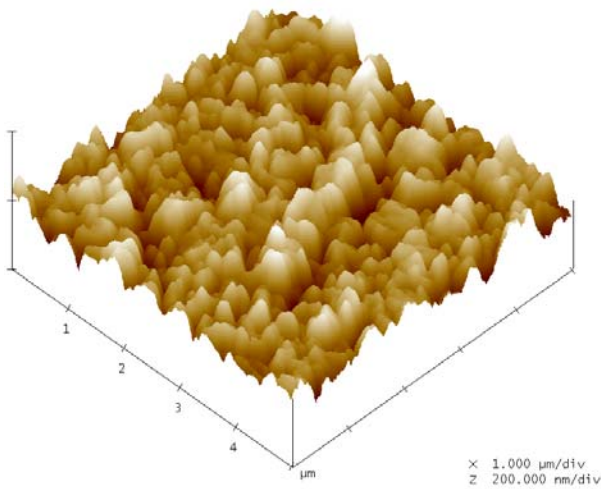
Digital Instruments NanoScope
 Scan size 5.000 μm
 Scan rate 1.907 Hz
 Number of samples 512
 Image Data Height
 Data scale 200.0 nm
 Engage X Pos
 Engage Y Pos



@ 140°C

RMS = 21.119nm

Thickness = 209nm

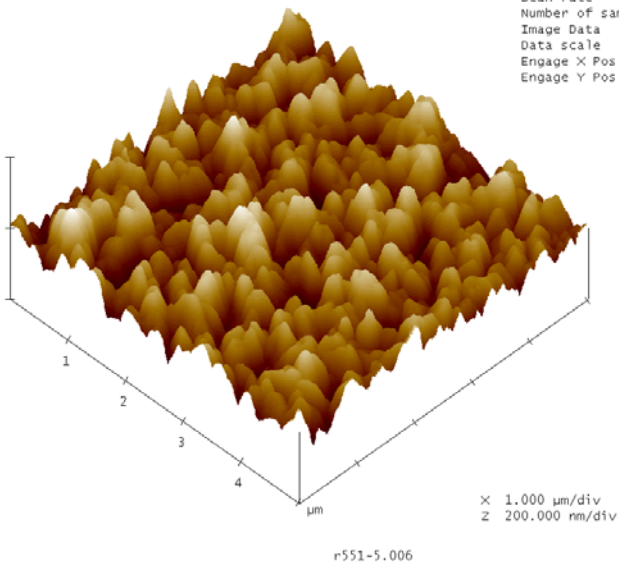


@ 160°C

RMS = 25.132nm

Thickness = 345nm

Digital Instruments NanoScope
 Scan size 5.000 μm
 Scan rate 1.907 Hz
 Number of samples 512
 Image Data Height
 Data scale 200.0 nm
 Engage X Pos
 Engage Y Pos



@ 180°C

RMS = 30.636nm

Thickness = 577nm

Fig. 4-9 AFM image showing surface roughness for Cu films deposited in a duration of 10 min on $\text{C}_2\text{H}_5\text{I}$ -treated TaN substrate at different temperatures.

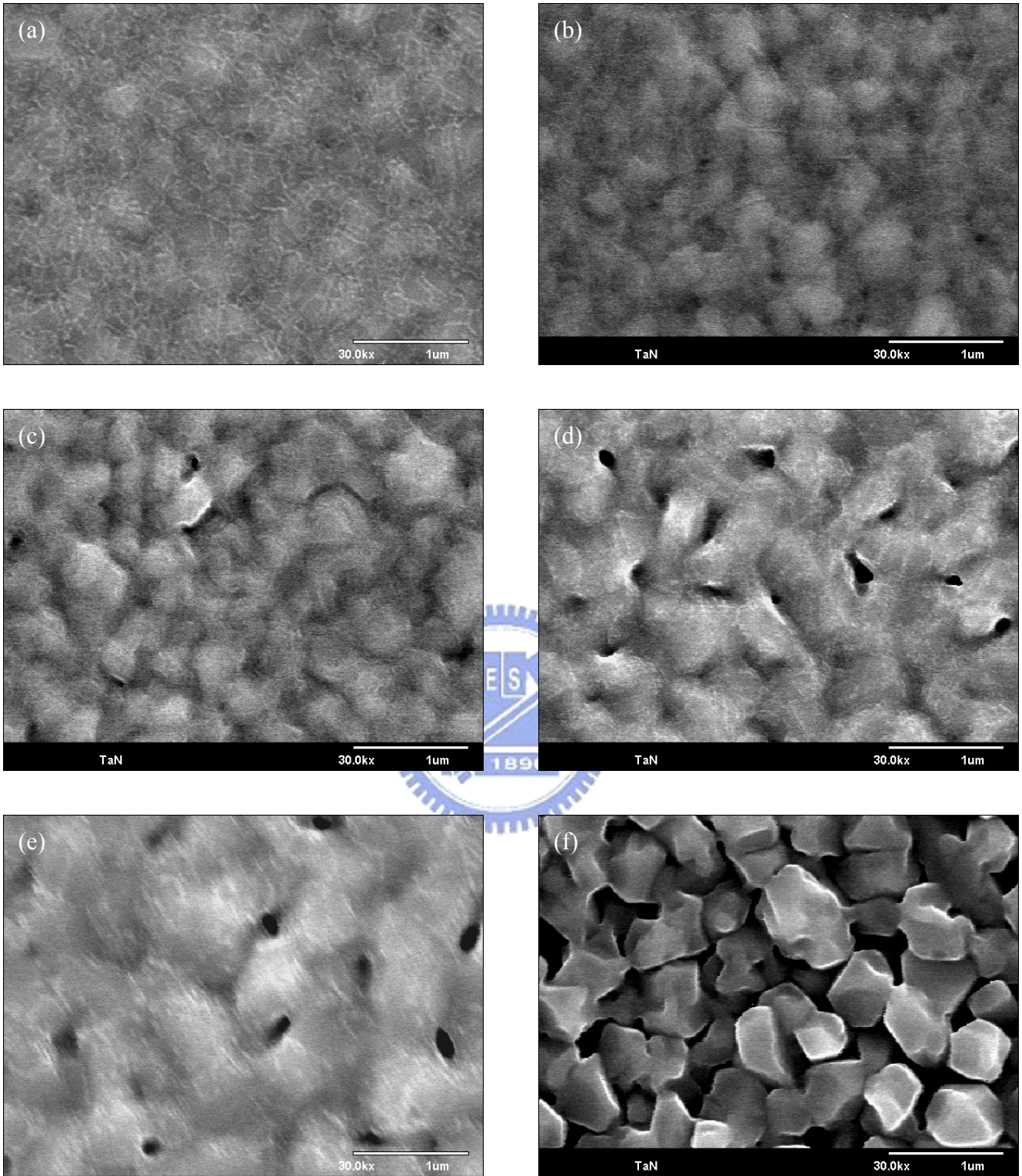


Fig. 4-10 SEM micrographs showing surface morphology of 400°C-annealed Cu films deposited on control TaN substrate at (a) 140°C, (b) 160°C, (c) 180°C, (d) 200°C, (e) 220°C, and (f) 240°C.

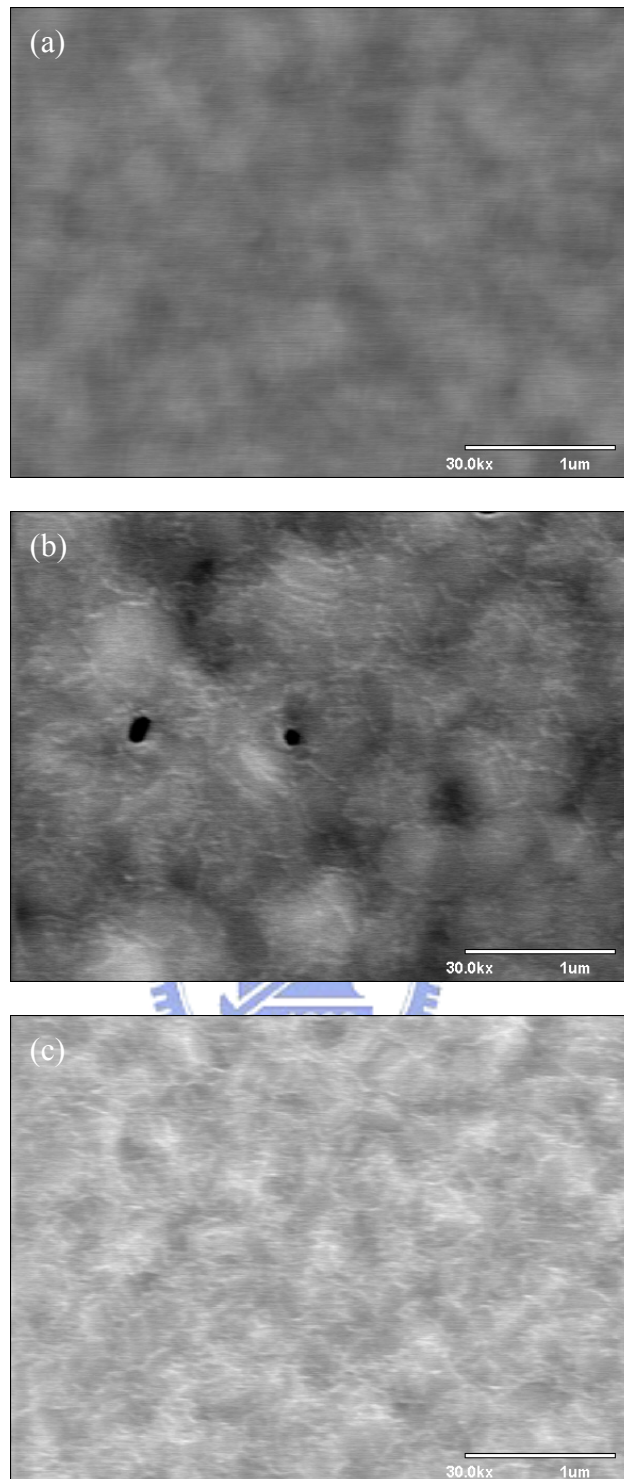
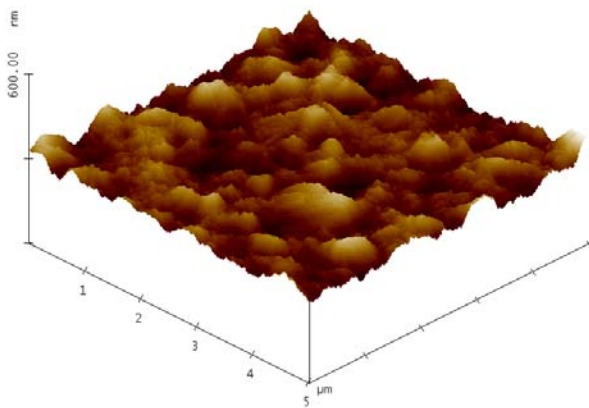
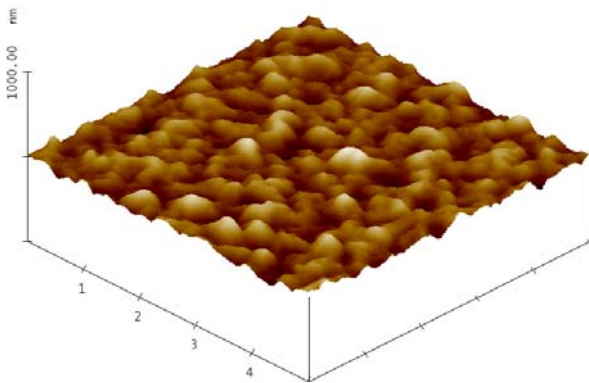


Fig. 4-11 SEM micrographs showing surface morphology of 400°C-annealed Cu films deposited on C₂H₅I-treated TaN substrate at (a) 140°C, (b) 160°C, and (c) 180°C



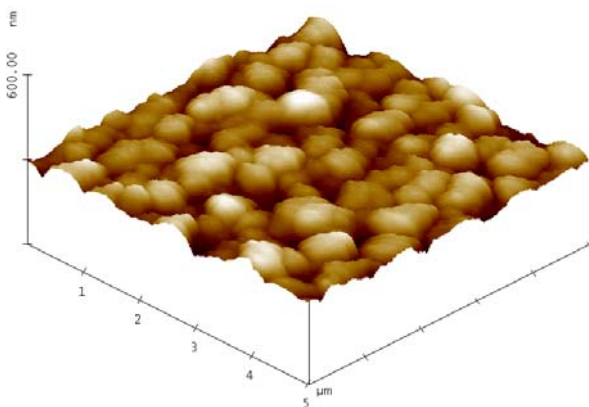
@ 140°C

RMS = 18.53nm



@ 160°C

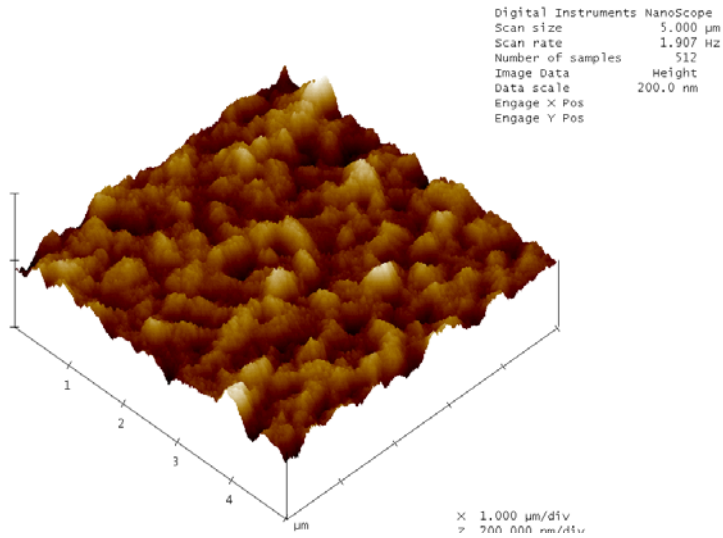
RMS = 20.47nm



@ 180°C

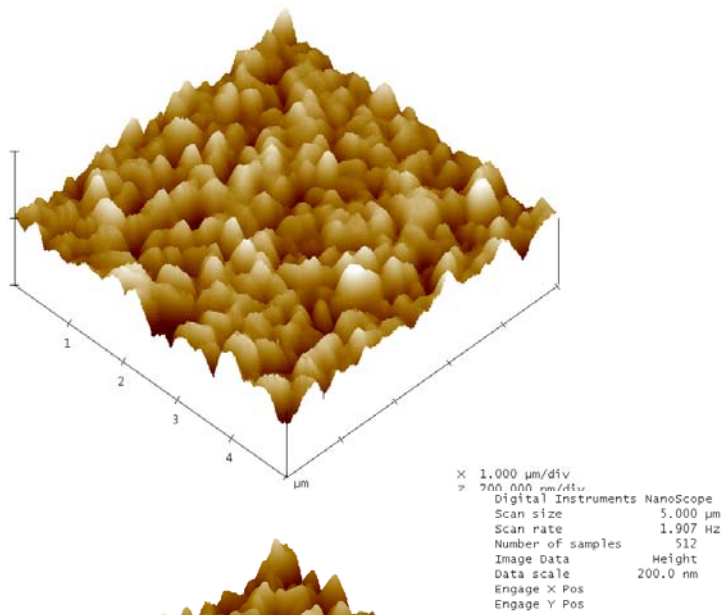
RMS = 25.68nm

Fig. 4-12 AFM image showing surface roughness of 400°C-annealed Cu films deposited on control TaN substrate at different temperatures.



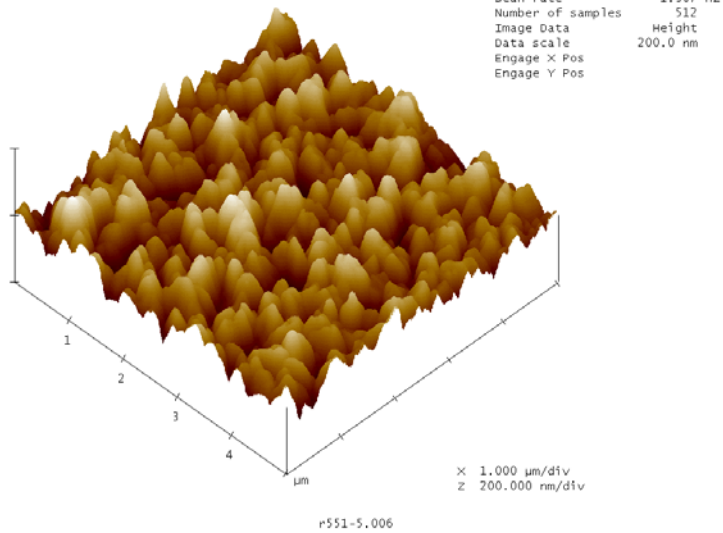
@ 140°C

RMS = 15.13nm



@ 160°C

RMS = 20.43nm



@ 180°C

RMS = 25.57nm

Fig. 4-13 AFM image showing surface roughness of 400°C-annealed Cu films deposited on $\text{C}_2\text{H}_5\text{I}$ -treated TaN substrate at different temperatures.

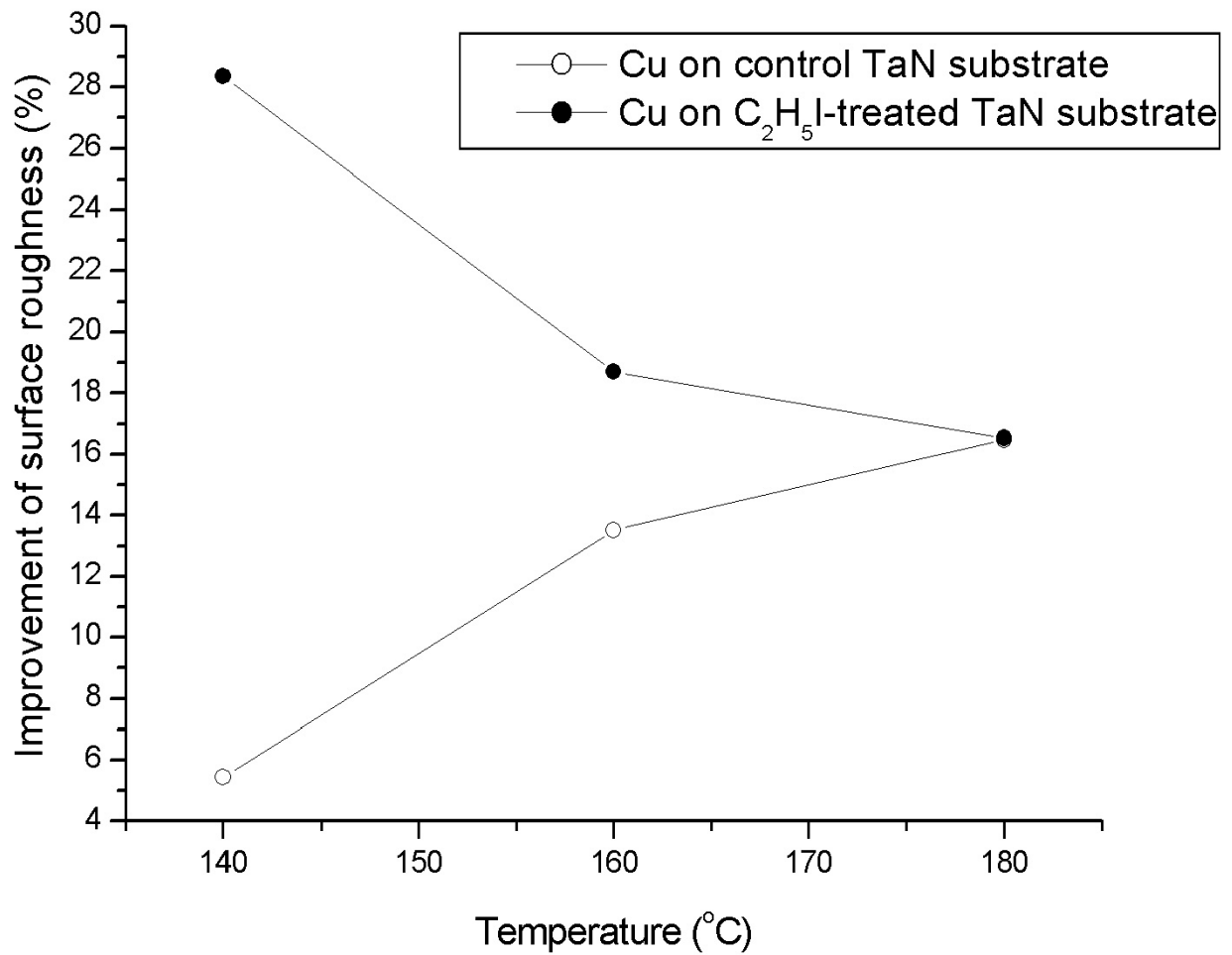


Fig. 4-14 Improvement of surface roughness vs. deposition temperature for Cu films deposited on TaN substrate with and without C₂H₅I treatment after 400°C thermal annealing.

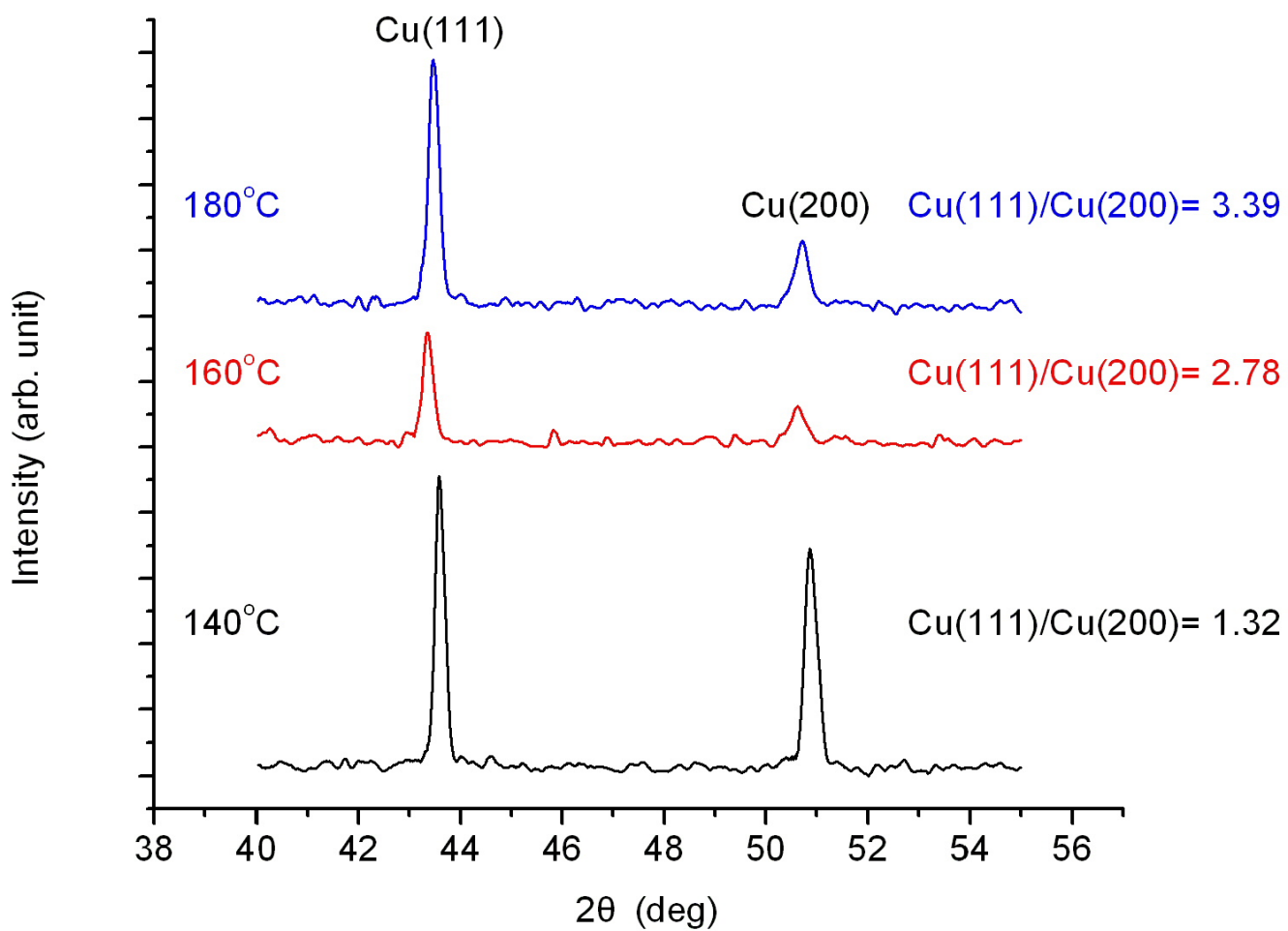


Fig. 4-15 XRD spectra of 400°C-annealed Cu films deposited on control TaN substrate at different temperatures.

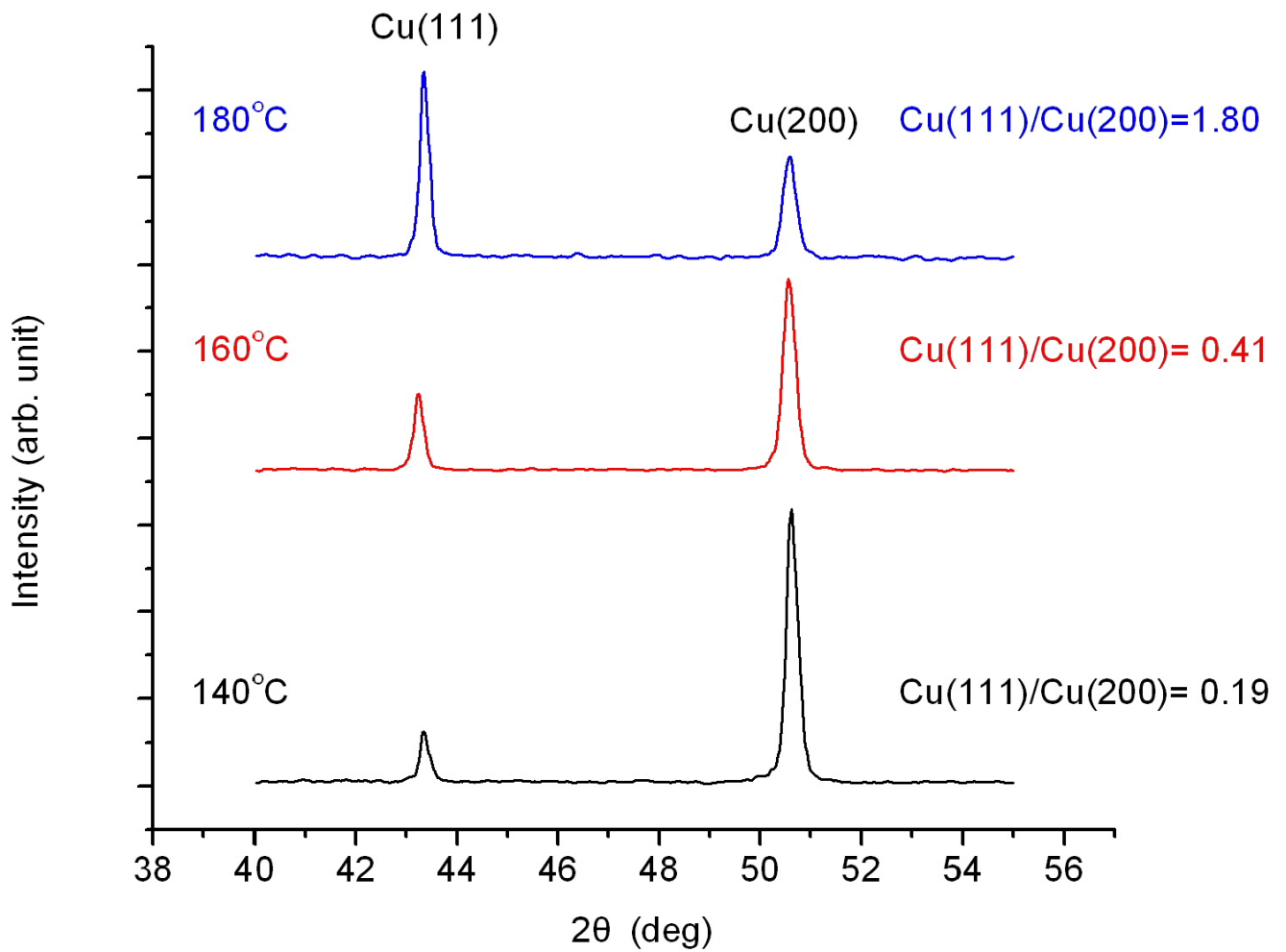


Fig. 4-16 XRD spectra of 400°C-annealed Cu films deposited on C₂H₅I-treated TaN substrate at different temperatures.

Chapter 5

Via-Filling of Cu CVD on Via-Patterned Substrate with TaN Liner

5.1 Introduction

The Cu damascene scheme has been developed to implement the multilevel interconnect of Cu lines in integrated circuits. The Cu ECD combined with the ionized metal plasma (IMP) PVD of a thin Cu seed layer and barrier layer provides a viable solution for IC technologies above $0.13\mu\text{m}$; however, the technique of this method will face more stringent challenge because of the requirement of a more stringent conformal and continuous thin barrier as well as conformal and void-free Cu film filling into deep sub-quarter micron vias for the IC technology beyond $0.13\mu\text{m}$ [32]. Although the traditional Cu CVD method easily results in a seam inside the vias and trenches due to the conformal deposition, it has been reported that vias/trenches could be filled with Cu in a bottom-up fashion (superfilling), resulting in a seam-free filling [13, 14]. This technique used iodine as catalytic surfactant to carry out the bottom-up superfilling. In this chapter, we investigate the via-filling behavior of Cu CVD using iodoethane ($\text{C}_2\text{H}_5\text{I}$) as catalyst surfactant.

5.2 Experimental Details

In this study, 25 nm-thick TaN layers were used as the diffusion barrier for the CVD of Cu films. To evaluate the via-filling capability of Cu CVD, two sets of vias of different feature sizes were patterned on 1- μm -thick fluorine doped

silicon glass (FSG) covered Si wafer. An IMP sputtering system was used to deposit conformal TaN layers of 25 nm thickness into the high aspect ratio (AR) vias. The diameters of the vias are 0.16 and 0.25 μm . In the real pattern, the patterned and measured error will be about several nanometers. The general processing conditions of Cu CVD for the study in this chapter are the same as those used in chapter 3, as shown in Table 3-1, except the deposition pressure and the flow rate of carrier gas (helium). The deposition pressures used for via-filling of Cu film were 60 and 150 mtorr. In order to pump the pressure in the reaction chamber down to 60 mtorr, the flow rate of carrier gas was reduced to 13 sccm while the liquid precursor flow rate was maintained at 0.4 ml/min. For the Cu CVD run at 150 mtorr, the flow rate of He carrier gas was 25 sccm and the Cu precursor flow rate was maintained at the same value of 0.4 ml/min.

5.3 Via-Filling on Via-Patterned Substrate with TaN Liner

Via-filling behavior of Cu CVD was investigated at temperatures ranging from 140 to 200°C. At temperatures above 200°C, the Cu film deposition belongs to the mass-flow-controlled mechanism, and it is disadvantageous to via-filling [33]. Post via-filling thermal annealing was performed at 400°C for 30 min in N₂ ambient to improve the adhesion of Cu films to the TaN barrier layer and to eliminate the microvoids between Cu grains in the vias. Figure 5-1 illustrates the SEM micrographs showing cross-sectional views of via-filling for the 0.25- μm -diameter vias under 150 mtorr at various temperatures. It can be seen that at the deposition temperature of 160°C, the bottom of the vias can be filled. At the higher deposition temperatures of 180 and 200°C, presumably the growth rate of Cu film became too fast such that the top of the via was quickly obstructed

by the Cu film, resulting in failure of via-filling. For the case of via-filling at 140°C, it can be seen that Cu was able to reach the bottom of the via; however, the via-filling was apparently incomplete for the 10 min run presumably because of low deposition rate and long incubation time at the low deposition temperature of 140°C. Figure 5-2 illustrates the cross-sectional view SEM micrographs for the via-filling of the 0.16- μm -diameter vias under 150 mtorr at various temperatures. At the higher temperature of 180 and 200°C, Cu was not able to deposit inside these smaller vias; even at the lower temperatures of 160 and 140°C, Cu was not able to fill the vias at the bottom. It was reported that for the Cu CVD at high temperatures and high pressures, the reactive sticking coefficient of the precursor species is presumably too high such that the Cu containing species cannot reach the bottom of the smaller vias [31], such as the via-filling with Cu-CVD at 180 and 200°C and 150 mtorr studied in this work. At the lower temperatures of 160 and 140°C, the results of via-filling were apparently improved to some extent.

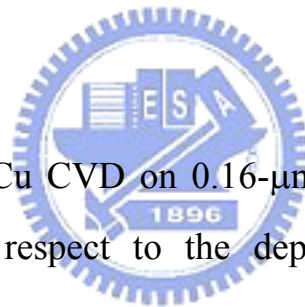
Figure 5-3 shows the cross-sectional view SEM micrographs for the via-filling of the 0.16- μm -diameter vias under 60 mtorr at 140 and 160°C. By comparing the results of via-filling shown in Fig. 5-2 and Fig. 5-3, we found clearly that reducing the deposition pressure (from 150 to 60 mtorr) and increasing the Cu precursor concentration in the carrier gas (from He flow rate of 25 to 13 sccm mixed with the same liquid Cu precursor of 0.4 ml/min) improved the via-filling capability, particularly at the lower deposition temperature of 140°C. From these experimental results, we may conclude that low pressure, low temperature, and high concentration of Cu containing species in the gas phase of CVD facilitate the via-filling.

5.4 Effect of C₂H₅I treatment on Via-Filling

Figure 5-4 illustrates the cross-sectional view SEM micrographs for the via-filling of the 0.16- μ m-diameter vias under 150 mtorr at various temperatures. The C₂H₅I treatment on the patterned substrate did improve the via-filling capability, as evidenced by comparing Fig. 5-4 and Fig. 5-2; the most obvious improvement can be found for the via-filling at the deposition temperature of 140°C. Figure 5-6 shows the cross-sectional view SEM micrographs for the via-filling of the 0.16- μ m-diameter vias under 60 mtorr at 140 and 160°C. Better result was obtained by using lower pressure (60 mtorr) and lower temperature (140°C) deposition.

5.5 Summary

Via-filling capability of Cu CVD on 0.16- μ m and 0.25- μ m vias with TaN liner was investigated with respect to the deposition conditions (including temperature, pressure, and Cu precursor concentration in the carrier gas) and the C₂H₅I catalyst effect. A better via-filling of Cu film can be achieved at low temperature and low pressure and high concentration of precursor species in the gas phase of Cu CVD. Substrate pretreatment by C₂H₅I catalyst resulted in improved via-filling capability under higher deposition pressure of 150 mtorr; however, the improvement in via-filling capability under deposition pressure of 60 mtorr and increased Cu precursor concentration in the gas phase of Cu CVD was not obvious. More effort is needed to clarify the role of C₂H₅I catalyst in sub-quarter-micron via-filling.



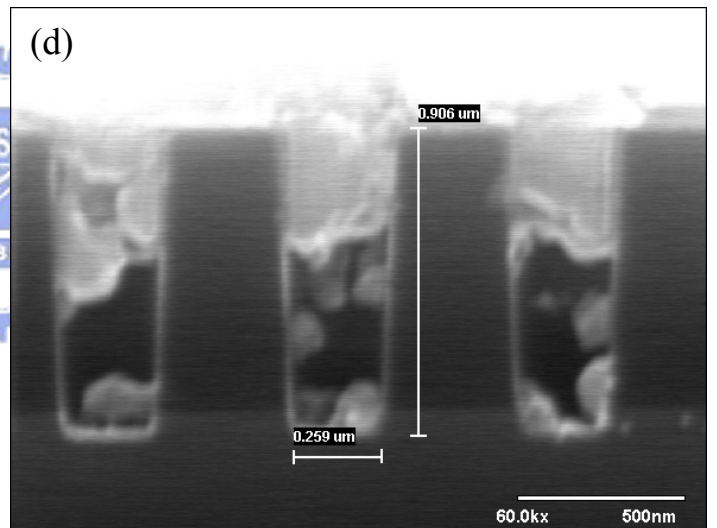
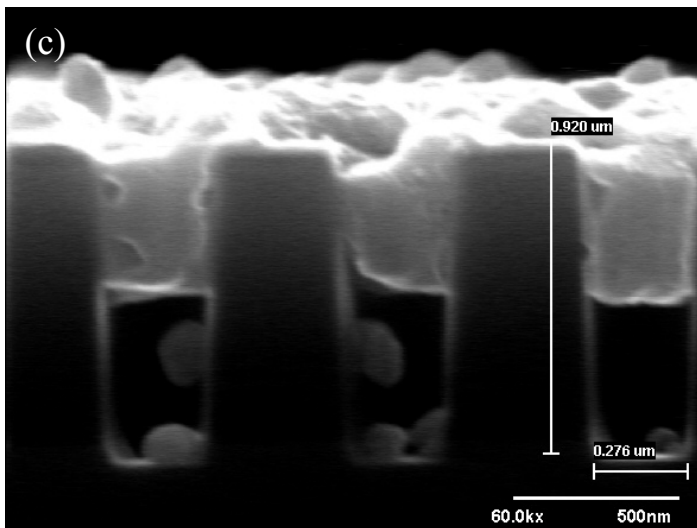
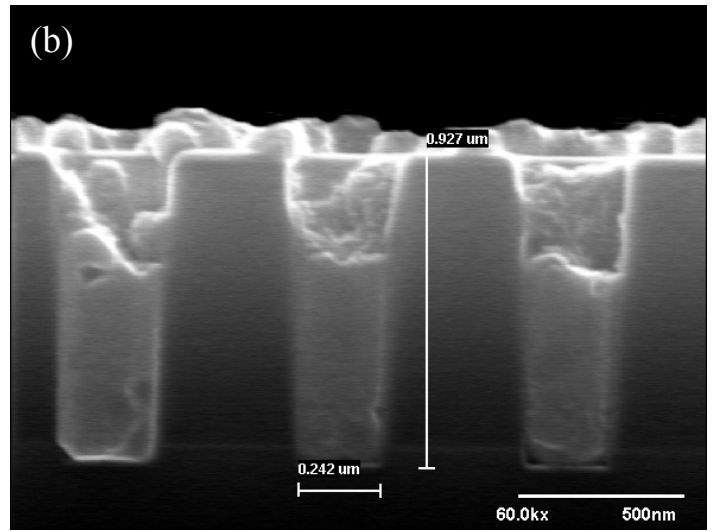
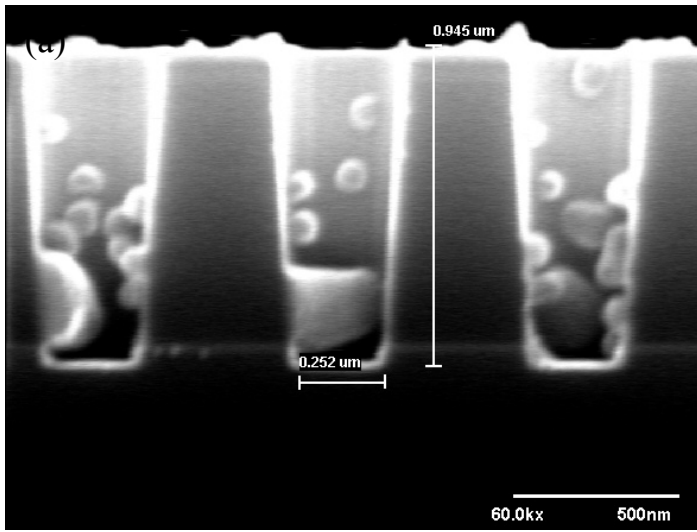


Fig. 5-1 SEM micrographs showing cross-sectional views of via-filling for 0.25- μ m-diameter vias under 150 mtorr at (a) 140°C, (b) 160°C, (c) 180°C, and (d) 200°C. The Cu CVD was conducted for 10 min for all samples.

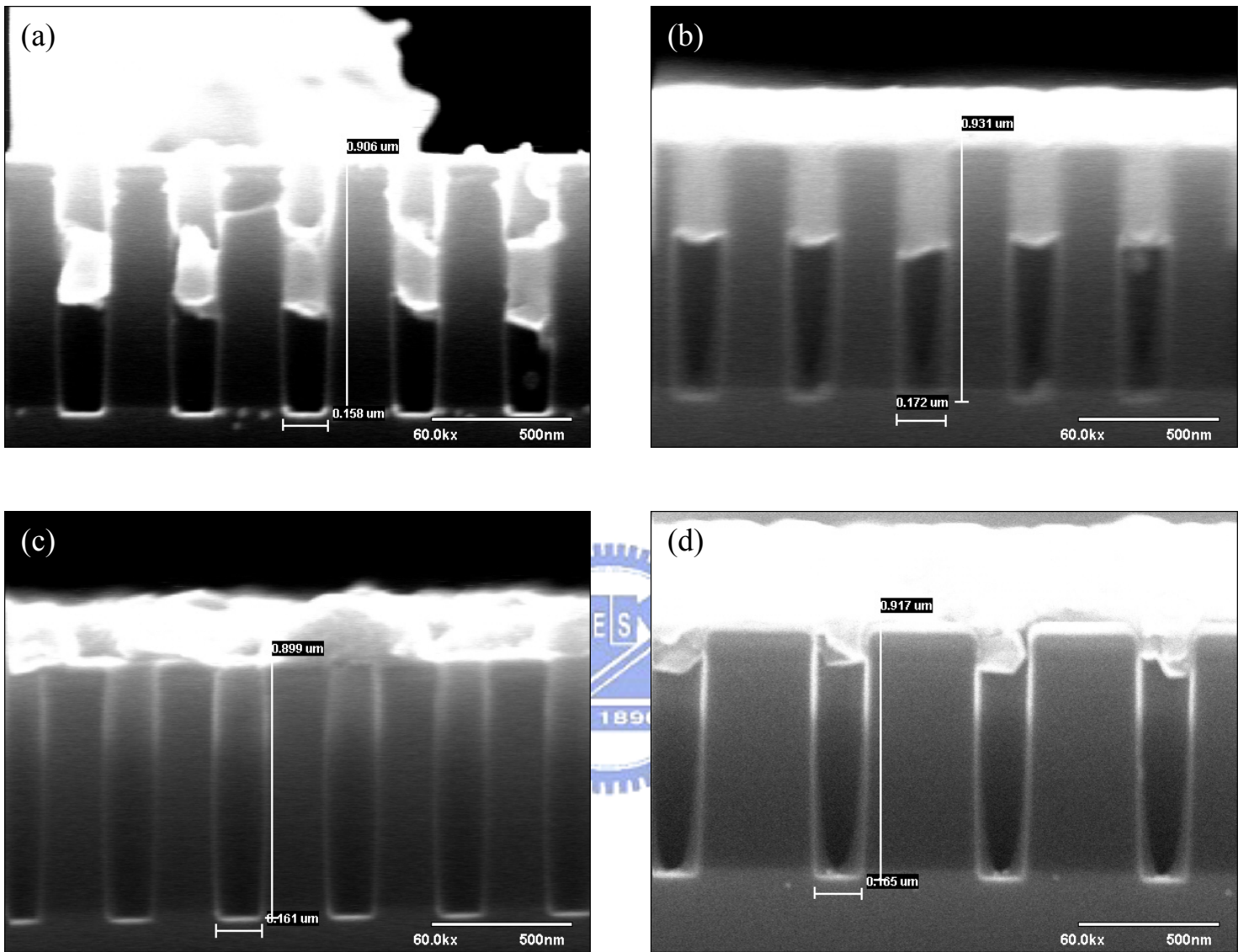


Fig. 5-2 SEM micrographs showing cross-sectional views of via-filling for 0.16- μm -diameter vias under 150 mtorr at (a) 140°C, (b) 160°C, (c) 180°C, and (d) 200°C. The Cu CVD was conducted for 10 min for all samples.

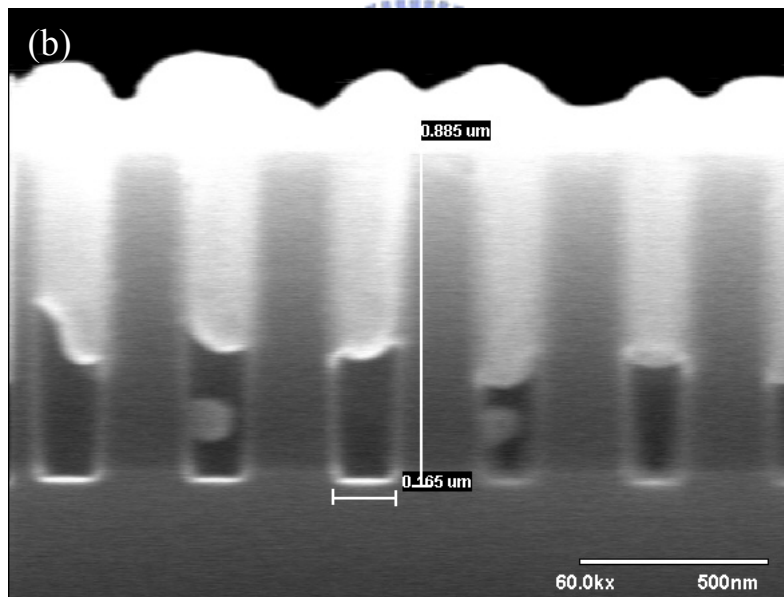
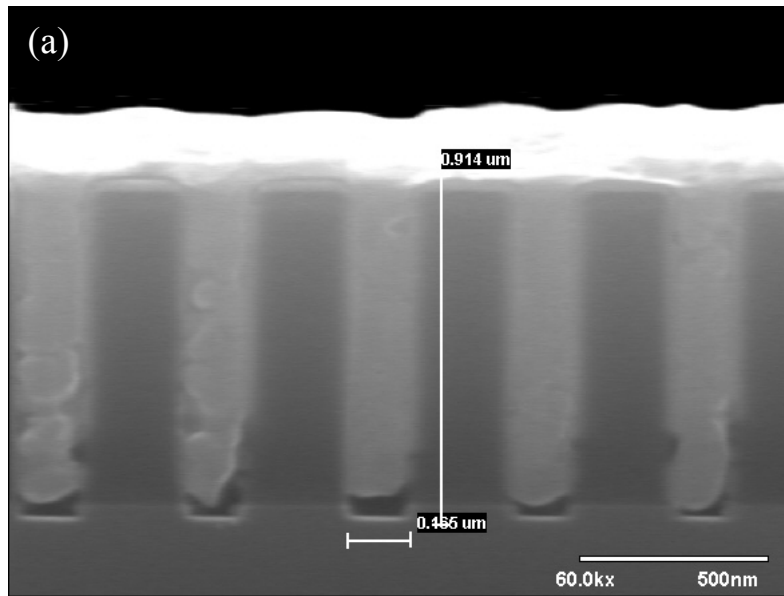


Fig. 5-3 SEM micrographs showing cross-sectional views of via-filling for 0.16- μm -diameter vias under 60 mtorr at (a) 140°C, and (b) 160°C. The Cu CVD was conducted for 10 min.

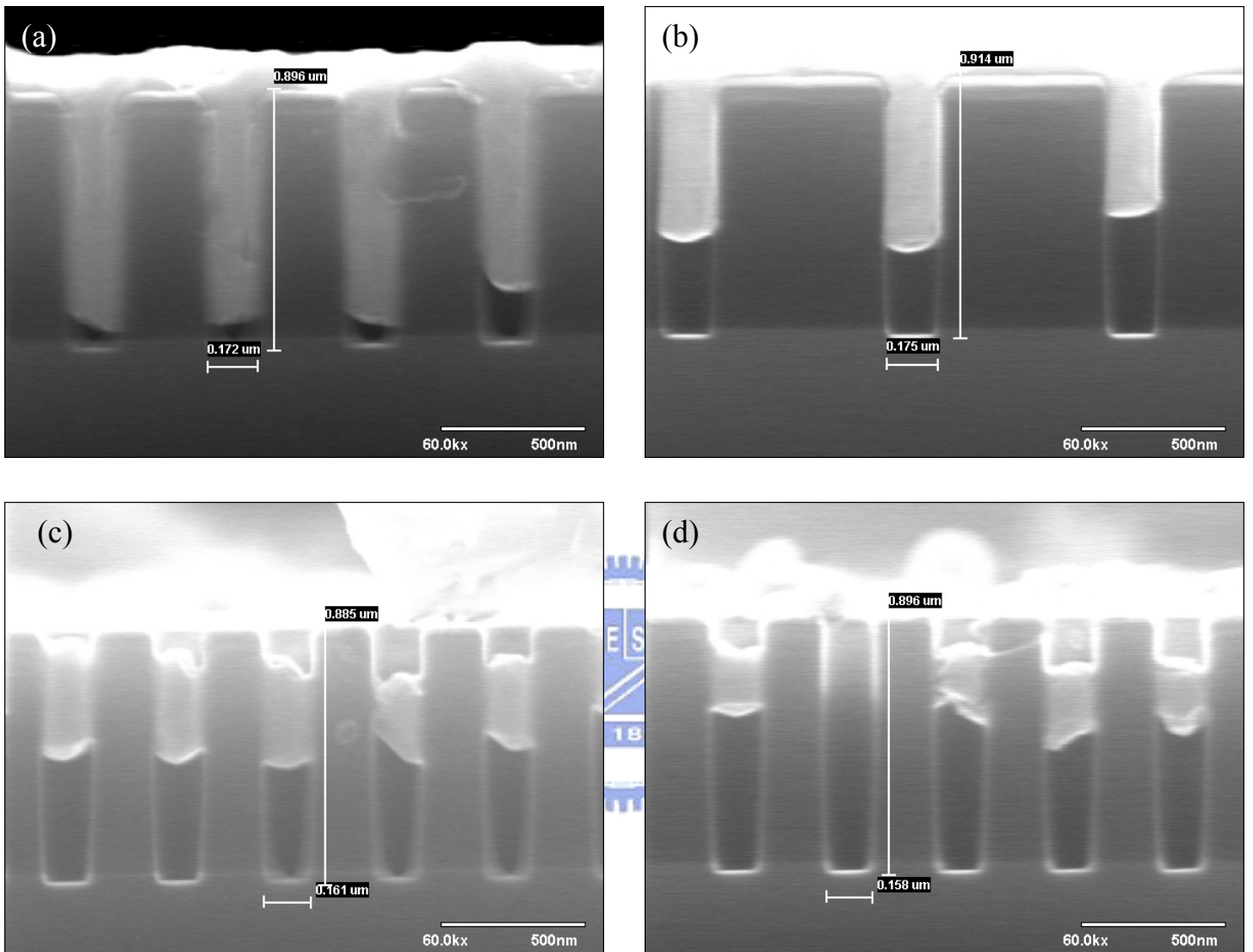


Fig. 5-4 SEM micrographs showing cross-sectional views of via-filling for 0.16- μm -diameter vias on $\text{C}_2\text{H}_5\text{I}$ -treated patterned substrate under 150 mtorr at (a) 140 $^{\circ}\text{C}$, (b) 160 $^{\circ}\text{C}$, (c) 180 $^{\circ}\text{C}$, and (d) 200 $^{\circ}\text{C}$. The Cu CVD was conducted for 10 min for all samples.

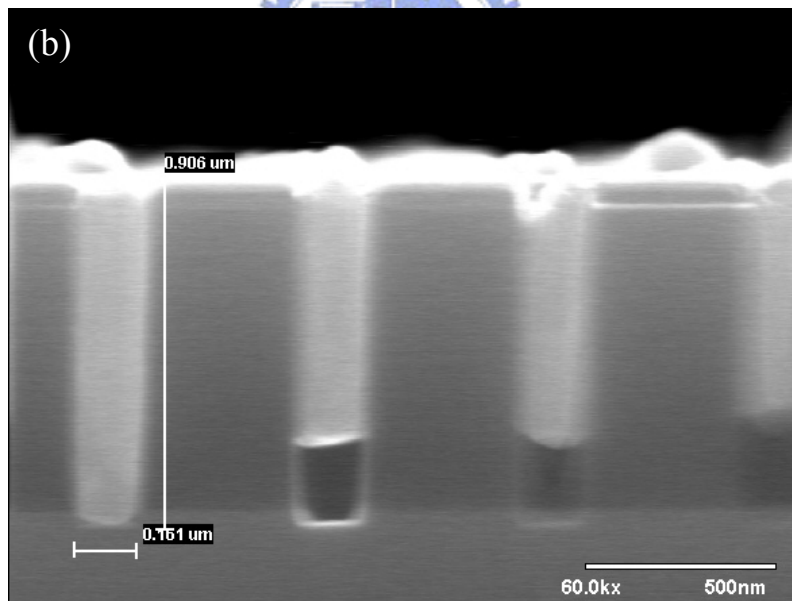
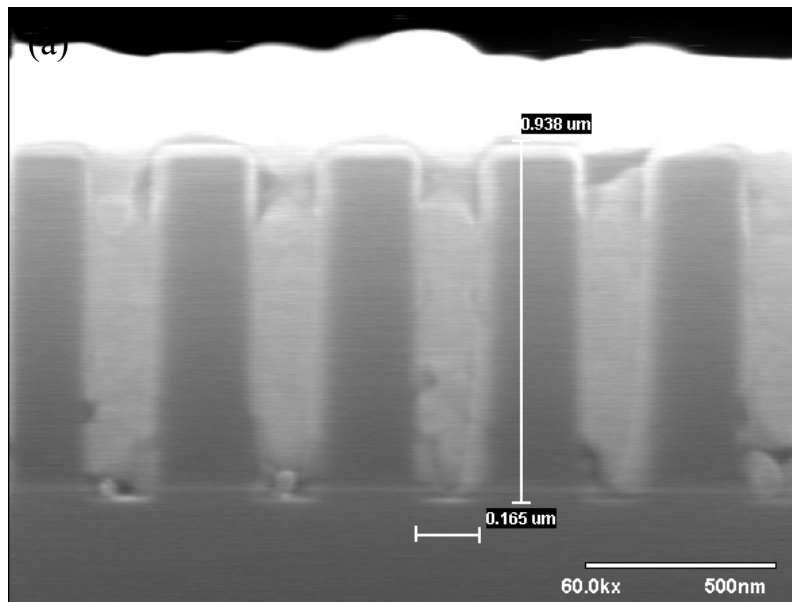


Fig. 5-5 SEM micrographs showing cross-sectional views of via-filling for 0.16- μm -diameter vias on $\text{C}_2\text{H}_5\text{I}$ -treated patterned substrate under 60 mtorr at (a) 140°C , and (b) 160°C . The Cu CVD was conducted for 10 min.

Chapter 6

Conclusion and Suggestions for Future Work

6.1 Conclusion

This thesis studies the effects of C_2H_5I catalyst on the Cu chemical vapor deposition, including Cu nucleation, Cu film property, and via-filling capability. Sputter-deposited TaN was used as the substrate for the Cu CVD and the vapor phase C_2H_5I was used for TaN surface treatment prior to the Cu CVD.

The substrate pretreatment by the vapor phase C_2H_5I enhanced the adsorption of Cu species on the substrate surface, reduced the incubation time of nucleation, and thus accelerated the Cu film formation. The wetting angle of Cu grains nucleated on the C_2H_5I -treated TaN substrate surface was larger than that nucleated on the control TaN substrate (63° vs. 94°). As a result, it also promoted vertical growth of the Cu film, degraded film adhesion to the substrate, and enhanced (200)-preferred orientation packed configuration in comparison with the Cu film deposited on the control TaN substrate.

The CVD Cu films on the C_2H_5I -treated TaN substrate have a higher deposition rate and lower film resistivity; however, they also have a lower intensity peak ratio of Cu(111) to Cu(200) reflections and a degraded adhesion to the TaN substrate. Post-deposition thermal annealing at 400°C in N_2 ambient was able to further reduce the film resistivity and surface roughness as well as slightly improve the adhesion to the TaN substrate.

Via-filling capability of Cu CVD on 0.25- and 0.16- μm -diameter vias with TaN liner was investigated. It is found that notable improvement in via-filling

capability of Cu CVD can be achieved at low deposition temperature (as low as 140°C), low deposition pressure, and high concentration of precursor species in the gas phase of CVD. Unfortunately, via-filling capability of Cu CVD by using vapor phase C_2H_5I substrate did not exhibit an obvious improvement. More effort is needed to understand the role of C_2H_5I catalyst in the process of Cu CVD.

6.2 Suggestions for Future Work

There are a number of Cu-CVD related topics which are worthy of suggestion for future work as follows.

- (1) Stress-temperature behavior of CVD-Cu film deposited on C_2H_5I -treated diffusion barrier substrates.
- (2) Effects of I_2 -plasma substrate treatment on CVD-Cu films.
- (3) Effects of plasma substrate treatment on selective Cu CVD.
- (4) Effects of combined plasma and catalyst substrate treatment on CVD-Cu films.
- (5) Effects of plasma substrate treatment on via/trench filling of Cu CVD.

References

- [1] R. Liu, C. S. Pai, and E. Martinez, *Solid State Electron.*, **43**, 1003 (1999).
- [2] C. K. Hu and J. M. E. Harper, *Mater. Chem. Phys.*, **52**, 5 (1998).
- [3] R. J. Gutmann, T. P. Chow, A. E. Kaloyeros, W. A. Lanford, and S. P. Murarka, *Thin Solid Films*, **262**, 177 (1995).
- [4] N. Awaya, H. Inokawa, E. Yamamoto, Y. Okazaki, M. Miyake, Y. Arita, and T. Kobayashi, *IEEE Trans. Electron Devices*, **43**, 1206 (1996).
- [5] J. P. O’Kella, K. F. Mongey, Y. Gobil, J. Torres, P. V. Kelly, and G. M. Crean, *Microelectron. Eng.*, **50**, 473 (2000).
- [6] J. C. Chiou, K. C. Juang, and M. C. Chen, *J. Electrochem. Soc.*, **142**, 177 (1995).
- [7] J. C. Chiou, Y. J. Chen, and M. C. Chen, *J. Electron. Mater.*, **23**, 383 (1994).
- [8] C. K. Hu, B. Luther, F. B. Kaufman, J. Hummel, C. Uzoh, and D. J. Pearson, *Thin Solid Films*, **262**, 84 (1995).
- [9] A. L. S. Loke, C. Ryu, C. P. Yue, J. S. H. Cho, and S. S. Wong, *IEEE Electron Device Lett.*, **17**, 549 (1996).
- [10] J. C. Chiou, H. I. Wang, and M. C. Chen, *J. Electrochem. Soc.*, **143**, 990 (1996).
- [11] A. Jain and T. T. Kodas, *J. Vac. Sci. Technol. B*, **11**, 2107 (1993).
- [12] H. K. Liou, J. S. Huang, and K. N. Tu, *J. Appl. Phys.*, **77**, 5443 (1995).
- [13] K. C. Shim, H.B. Lee, O. K. Kwon, H. S. Park, W. Koh, and S. W. Kang, *J. Electrochem. Soc.*, **149**, G109 (2002).
- [14] H. Park, W. Koh, S. M. Choi, K. C. Park, H. K. Kang, and J. T. Moon, *Proceedings of IEEE 2001 International Interconnect Technology Conference (IITC)*, p.12 (2001).
- [15] E. S. Hwang and J. Lee, *Chem. Mater.*, **12**, 2076 (2000).

- [16] E. S. Hwang and J. Lee, *Electrochem. Solid State Lett.*, **3**, 138 (2000).
- [17] S. Wolf and R. N. Tauber, *Silicon Processing for the ULSI Era, Volume 1: Process Technology*, (Lattice press, 1986), Chap 16.
- [18] S. Hymes, K. S. Kumar, S. P. Murarka, W. Wang, and W. A. Lanford, *J. Vac. Sci. Technol. B*, **16**, 1107 (1998).
- [19] S. K. Young, D. Jung, and S. K. Min, *Thin Solid Films*, **349**, 36 (1999).
- [20] Y. K. Chae, Y. Shimogaki, and H. Komiyama, *J. Electrochem. Soc.*, **145**, 4226 (1998)
- [21] D. H. Kim, R. H. J. Wentorf, and W. N. Gill, *J. Appl. Phys.*, **74**, 5164 (1993).
- [22] K. Hanaoka, H. Ohnishi, and K. Tachibana, *Jpn. J. Appl. Phys.*, **34**, 2430 (1995).
- [23] K. Kamoshida and Y. Ito, *J. Vac. Sci. Technol. B*, **15**, 961 (1997).
- [24] C. L. Chang, Master Thesis, National Chiao Tung University, Taiwan (2003).
- [25] K. S. Hwang, J. H. Lee, D. S. Yoon, I. Han, J. H. Noh, J. H. Park, and T. S. Kim, *Journal of the Korean Physical Society* (2004).
- [26] Y. Qian, C. Y. Li, L. T. Koh, J. J. Wu, and J. Xie, *Proceedings of 1999 VLSI Multilevel Interconnection Conf. (VMIC)*, p.558 (1999).
- [27] R. Kroger, M. Eizenberg, D. Cong, N. Yoshida, L. Y. Chen, S. Ramaswami, and D. Carl, *Microelectron. Eng.*, **50**, 375 (2000).
- [28] N. I. Cho and Y. Sul, *Mater. Sci. Eng. B*, **72**, 184 (2000).
- [29] S. S. Yoon, J. S. Min, and J. S. Chun, *J. Mater. Sci.*, **30**, 2029 (1995).
- [30] P. J. Lin and M. C. Chen, *Jpn. J. Appl. Phys.*, **38**, 4863 (1999).
- [31] C. L. Lin, Ph.D Dissertation, National Chiao Tung University, Taiwan, (2002).
- [32] P. Motte, M. Proust, J. Torres, Y. Gobil, Y. Morand, J. Palleau, R. Pantel, and M. Juhel, *Microelectron. Eng.*, **50**, 369 (2000).
- [33] A. Kobayashi, A. Sekiguchi, and O. Okada, *Jpn. J. Appl. Phys.*, **37**, 6358 (1998).